Multi-Dimensional Resource Allocation for Uplink Throughput Maximisation in Integrated Data and Energy Communication Networks

JIANJUN YANG[1], JIE HU [1], (Member, IEEE), KESI LV[1], QIN YU[1], (Member, IEEE), AND KUN YANG [1,2], (Senior Member, IEEE)

[1]School of Information and Communication Engineering, University of Electronic Science and Technology of China, Chengdu 611731, China
[2]School of Computer Science and Electronic Engineering, University of Essex, Colchester CO4 3SQ, U.K.

Corresponding author: Jie Hu (hujie@uestc.edu.cn)

ABSTRACT The interdisciplinary research of the radio-frequency (RF) signal-based wireless power and information transfer is expected to address the energy shortage issue in the massively deployed low-power Internet of Things devices. Different from conventional wireless powered communication networks (WPCNs), the hybrid base station (H-BS) adopts the simultaneous wireless information and power transfer (SWIPT) for the sake of satisfying the downlink data and energy requests of the multiple user equipments (UEs). The energy harvested from the downlink transmissions can be depleted for supporting the UEs' uplink transmissions. Integrating SWIPT in the downlink transmission of the WPCN yields a generic integrated data and energy communication network, where the H-BS is equipped with multiple antennas and both the downlink and uplink transmissions are slotted in the time-domain. Furthermore, both the sum-throughput and the fair-throughput of the uplink transmissions are maximized by jointly optimizing the transmit beamformer of the H-BS in the spatial-domain, the time-slot allocation in the time-domain and the signal splitting strategies of the UEs in the power domain, while satisfying the UEs' minimum downlink transmission requirements. Due to the non-convexity of the problem, a low-complexity successive convex approximation-based algorithm is relied upon for obtaining the optimal resource allocation scheme in the time-domain, power-domain, and spatial-domain. The numerical results validate the efficiency of our proposed resource allocation algorithm and they also demonstrate that supporting low-rate data services during the downlink transmissions does not degrade the wireless power transfer and hence does not reduce the uplink throughput.

INDEX TERMS Simultaneous wireless information and power transfer (SWIPT), wireless powered communication network (WPCN), integrated data and energy communication network (IDEN), multiple antennas, multi-dimensional resource allocation, sum-throughput maximisation, fair-throughput maximisation, successive convex approximation (SCA).

NOMENCLATURE

CSI	Channel State Information
DC	Direct Current
H-BS	Hybrid Base Station
IDEN	Integrated Data and Energy communication Network
IoT	Internet of Things
RF	Radio Frequency
SCA	Successive Convex Approximation
SDR	Semi-Definite Relaxation
SWIPT	Simultaneous Wireless Information and Power Transfer
TDD	Time Division Duplex
TDMA	Time Division Multiple Access
UE	User Equipment
WPCN	Wireless Powered Communication Network
WIT	Wireless Information Transfer
WPT	Wireless Power Transfer

I. INTRODUCTION

In the upcoming era of the Internet of Things (IoT) [1], the low power IoT devices are massively deployed for the sake of data collecting, environment sensing and decision making etc., which constitute the promising future of smart cities [2], industrial internet [3] and autonomous driving [4]. However, the functions of the low-power IoT devices are heavily restricted by the energy supply, since they are only powered by the batteries having limited capacity. Since the IoT devices are normally deployed in unreachable places, frequently replacing batteries may result in an escalating maintenance expenditure of the operator [5].

Harvesting energy from the renewable sources, such as sunlight, wind and tidal wave, is a feasible option for the sake of increasing the lifetime of the low-power user equipments (UEs) in wireless communication networks [6]. Furthermore, our environment is also full of electronic-magnetic signals emitted by various transmitters operating in the radio-frequency (RF) band [7]. The UEs can also harvest the energy of these RF signals for charging their batteries by converting the received RF signal to the direct current (DC). Muncuk *et al.* [8] designed an adjustable RF-DC converter operating in various RF spectral bands ranging from 700 MHz of LTE band and 850 MHz of GSM band to 900 MHz of ISM band. Their multi-band RF-DC converter can achieve at least 45 % energy conversion efficiency. Alevizos and Bletsas [9] studied both the sensitivity and the non-linearity of RF-DC converters and quantified their effect on the performance of RF energy harvesting. However, energy harvesting is self-initiated by UEs, who are running out of energy. Moreover, UEs are only capable of passively gleaning energy from the environment, which results in low-efficiency, unpredictability and uncontrollability of the stochastic energy arrivals. In order to increase the UEs' energy harvesting efficiency, RF signals can be exploited for enabling the dedicated wireless power transfer (WPT). For example, Grover and Sahai [10] optimised the WPT performance in a single-input-single-output frequency selective channel.

The downlink RF signal based WPT is enabled for the sake of supporting the low-power UEs' uplink transmission, which stimulates substantial research interests in the design of wireless powered communication networks (WPCNs) [11]–[21]. A hybrid base station (H-BS) plays an central role in WPCNs, which both supports the downlink WPT and the uplink data reception. The "harvest-then-transfer" protocol has been adopted by the UEs for dividing the downlink WPT and the uplink wireless information transfer (WIT) in the time-domain [11].

However, the main challenge that deters WPCNs to become an reality is the lack of efficient resource allocation schemes for striking a balanced performance between the downlink WPT and the uplink WIT. Therefore, Ju and Zhang [12] studied a time-division-multiple-access (TDMA) protocol enabled WPCN and they optimised the time-domain resources for maximising the uplink sum-throughput, where the H-BS operates in

a half-duplex mode. Furthermore, Ju and Zhang [13] also studied the full-duplex aided WPCN. They proposed an optimal power and time allocation scheme for the sake of maximising the weighted uplink sum-throughput by considering both the perfect and imperfect self-interference cancellation. Che *et al.* [14] analyzed the spatial throughput performance in a large-scale WPCN by exploiting the classic stochastic geometry. In order to overcome the doubly near-far effect, which will be introduced at the beginning of Section IV, Chen *et al.* [15] proposed a pricing scheme to encourage the user cooperation in a WPCN for the sake of improving the performance of the uplink transmission.

Apart from the conventional uplink throughput maximisation [12]–[15], the energy efficiency of WPCNs have also attracted substantial research interest. For instance, Wu *et al.* [16] proposed an optimal time and power allocation scheme for maximizing the achievable energy efficiency of the WPCN studied by also considering the initial battery states of the UEs. Zewde and Gursoy [17] proposed an optimal resource allocation scheme for maximizing the effective energy efficiency of the WPCN studied, where the UEs adopts the power-domain non-orthogonal-multiple-access protocol for supporting their uplink transmissions.

Furthermore, multiple antennas equipped at H-BSs may provide additional degree of freedom in the spatial domain, which thus substantially improve the performance of the WPCNs. For instance, Huang *et al.* [18] derived the closed-form expression and the asymptotic expression in the high signal-to-noise-ratio region of a single UE's uplink throughput, which is powered by a H-BS equipped with multi-antennas in a WPCN. Furthermore, Liu *et al.* [19] propose an optimal downlink energy beamforming for the multi-antenna aided H-BS in order to maximise the minimum uplink throughput of the UEs in the WPCN. Ku and Lai [20] proposed a joint beamforming and time allocation scheme for maximizing the sum-throughput of the wireless powered device-to-device communication pairs. Moreover, Yuan *et al.* [21] studied an cluster based cooperation in a WPCN, where the multi-antenna of the H-BS is exploited for efficiently beaming the energy to the cluster heads.

In the conventional WPCNs [11]–[21], the downlink transmission of a H-BS completely contributes to the dedicated WPT, which largely ignores the downlink data requests of the UEs. However, coordinating the WPT and the conventional WIT in the same RF band is challenging, since they may compete for the precious resources of the air interface, which yields a large body of research concerning the simultaneous wireless information and power transfer (SWIPT) [22]–[27]. Varshney *et al.* [22] is the pioneer of exploring the inherent tradeoff between the WPT and the WIT from the information theoretical aspect by invoking an ideal receiver. In order to further advance the SWIPT to the practical implementation, signal splitting based receivers have been widely investigated. Zhou *et al.* [23] proposed practical receiver architectures for simultaneous reception

of the information and energy, which rely upon the signal splitting in either the power domain and the time-domain. Moreover, Xiong *et al.* [24] studied the rate-energy region of both the power splitting and time switching aided SWIPT receiver by taking the non-linearity of the RF-DC converter into account. Lee *et al.* [25] jointly optimized the transmit covariance matrices at the transmitter and the signal splitting ratios in the time-domain[1] at the receivers in order to achieve the boundary points of the rate-energy region and to minimize the transmit energy consumption. Furthermore, Xu *et al.* [26] utilized the power splitting based SWIPT receiver at the low-power UEs for simultaneous energy harvesting and the beam-domain channel estimation, which is relied upon for scheduling the uplink transmissions of the UEs. Mishra and Alexandropoulos [27] proposed an optimal transmit precoding scheme of the multi-antenna aided transmitter and an optimal power splitter of the SWIPT receiver, which is capable of maximizing the amount of energy harvested by the receiver. It has been widely recognised that the power splitting based receiver may reach a larger rate-energy region than its time switching based counterpart, when linear RF-DC converters are adopted [23] and [24].

Furthermore, Lv *et al.* [28] firstly integrate the SWIPT in the downlink transmission of the conventional WPCN. However, they mainly focus on the time-domain resource allocation for maximizing the uplink throughput performance by assuming a single antenna at the H-BS. Against this background, our novel contributions are summarized as below:

- *By integrating the SWIPT in the downlink transmission of the WPCN, we establish a generic Integrated Data and Energy communication Network (IDEN), where the UEs acquire both data and energy from the downlink transmission of the H-BS and they upload their own data to the H-BS by exploiting the energy harvested during their downlink transmissions.*
- *In order to maximise the sum-throughput and the fair-throughput of the UEs' uplink transmissions, the corresponding multi-dimensional resource allocation scheme is obtained by jointly optimizing the transmit beamformer of the H-BS in the spatial domain, by optimizing the time-slot allocation in the time-domain and by optimizing the UEs' power splitting strategies in the power domain.*
- *The original non-convex optimization problem is decomposed and transformed into several convex subproblems, which have been iteratively solved by exploiting the successive convex approximation (SCA) based algorithm for obtaining the optimal resource allocation scheme. The optimal initial transmit beamformer is found to significantly reduce the complexity of the SCA based algorithm.*
- *The numerical results demonstrate the efficiency of our proposed multi-dimensional resource allocation scheme*

and the advantage of our IDEN model over the conventional WPCN.

The rest of this paper is organized as follows. Our IDEN model is introduced in Section II, which is followed by the sum-throughput maximisation in Section III and the fair-throughput maximisation in Section IV, respectively. By providing the numerical results in Section V, we finally conclude this paper in Section VI.

II. SYSTEM MODEL

The IDEN system considered in our paper is illustrated in Fig.1, which consists of a single H-BS and a set of UEs $\mathcal{U} = \{U_i | i = 1, 2, \cdots, K\}$. The total number of UEs is thus $|\mathcal{U}| = K$. The H-BS equipped with N_t antennas has the following pair of functions:

- The H-BS transmits the modulated RF signals in the downlink by simultaneously delivering both the data and energy to the UEs;
- The H-BS receives the data uploaded by the UEs during their uplink transmissions.

The H-BS operates in a time-division-duplex (TDD) mode in order to avoid any potential interference between the downlink and uplink transmissions.
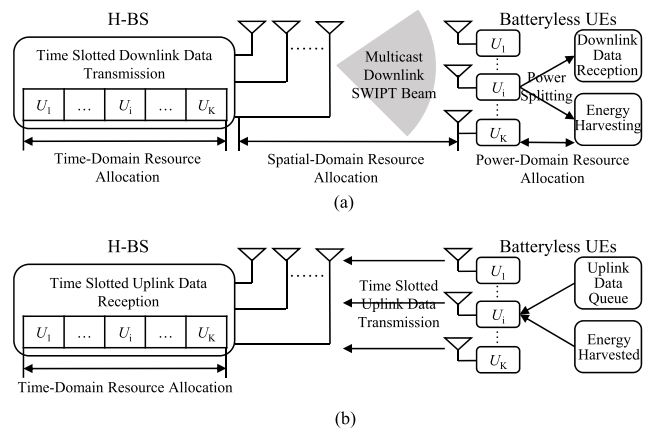

FIGURE 1. The (a) downlink and (b) uplink transmissions of the IDEN consisting of a single H-BS and K UEs.

The UEs in the IDEN system are batteryless but they are all equipped with super-capacitors. Their uplink transmissions completely rely on the energy harvested from the downlink transmissions of the H-BS. The UEs equipped with a single antenna has the following pair of functions:

- The modulated RF signals received by the UEs during the downlink transmission of the H-BS are split in the power domain in order to satisfy their data and energy requests. Specifically, all the UEs in the system have diverse downlink throughput requirements, which are denoted as $\mathcal{D} = \{D_i | i = 1, 2, \cdots, K\}$.
- Since super-capacitors have a very short discharging cycle, they cannot store energy for a long period. Therefore, the UEs may deplete all the energy harvested from the H-BS for powering their own uplink transmissions.
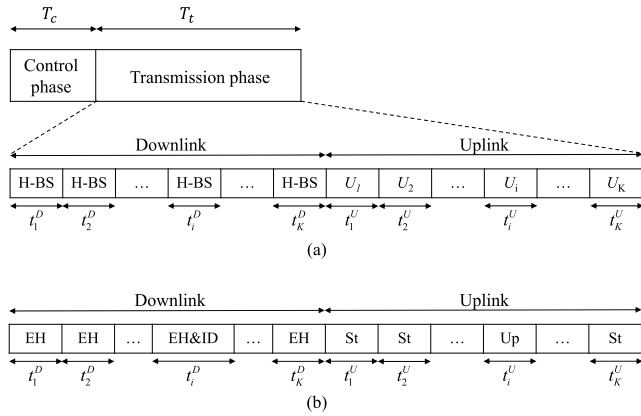
The UEs also operates in a TDD mode.

---

[1]This is also widely regarded as the time switching between the energy harvesting mode and the information decoding mode.

FIGURE 2. Frame structure of the (a) H-BS's and (b) UE's slotted operation. EH: Energy Harvesting. ID: Information Decoding. Up: Uploading. St: Standby.

A. FRAME STRUCTURE

In our IDEN system, the operations of both the H-BS and the UEs are slotted in the time-domain by adopting the classic TDMA protocol in order to suppress the interference incurred by the transmissions of multiple UEs [29]. In general, a single transmission frame consists of two phases, namely the control phase having a duration of T_c and the transmission phase having a duration of T_t, as depicted in Fig.2. Therefore, the duration of a single transmission frame is $T = T_c + T_t$. The control signalling exchange is carried out during the control phase in order to realize the following functions:

- *Channel Estimation*. A training pilot can be sent by a UE to the H-BS. The received pilot can be further processed by the H-BS in order to extract the channel state information (CSI) of the uplink between the UE and the H-BS. The acquired CSI of the uplink can also be regarded as that of the corresponding downlink by exploiting the channel reciprocity of the TDD system. This classic reverse-link training may significantly save the energy of the batteryless UEs, since the UE cannot afford neither sophisticated signal processing nor feedback transmission.
- *Resource Allocation*. Relying on the acquired CSI, the H-BS may carry out the resource allocation scheme in order to maximise the throughput performance. It then informs the UEs of their signal splitting strategies and the duration of their assigned time-slots.
- *Synchronization*. The H-BS and the UEs have to be accurately synchronized by invoking the time-stamp-based synchronization approach [30]. The clock information of the H-BS is broadcasted to the UEs during the control phase. The UEs may adjust their local clock to synchronize themselves with the UEs. Synchronization is particularly essential for the TDMA aided system.

The transmission phase is divided into a range of downlink time-slots denoted as $\mathbf{t}^D = \{t_j^D | j = 1, 2, \cdots, K\}$ for supporting the downlink transmissions of the H-BS and a range of uplink time-slots denoted as $\mathbf{t}^U = \{t_j^U | j = 1, 2, \cdots, K\}$ for supporting the uplink transmissions of the

multiple UEs. Therefore, we have

$$\sum_{i=1}^{K} (t_i^D + t_i^U) \leq T_t \qquad (1)$$

The detailed operations of the H-BS and the UEs during the transmission phase are portrayed in Fig.2 and summarized as below:

- For the downlink transmissions, the H-BS modulates the data requested by the UE U_i on the RF signal transmitted during the specific time-slot t_i^D, as illustrated in Fig.2(a). For the downlink reception, U_i split the received RF signal in the power-domain during t_i^D for simultaneous energy harvesting and information decoding. Due to the broadcast nature of the wireless channels, U_i may also harvest energy from the modulated RF signals requested by its peers during other time-slots, as illustrated in Fig.2(b).
- For the uplink transmissions, U_i may upload its data to the H-BS during the specific time-slot t_i^U, as depicted in Fig.2(a), by exploiting the energy harvested from all the time-slots $\mathbf{t}^D$. This is the classic "harvest-then-transfer" protocol [31]. During other time-slots of the uplink transmissions, U_i may remain in the standby mode without any other operation, as portrayed in Fig.2(b). The H-BS operates as a information receiver during the entire uplink transmission process.

B. CHANNEL MODEL

The far-field path-loss Ω_i between the H-BS and the UE U_i can be formulated as

$$\Omega_i = \Omega_0 \cdot \left(\frac{d_i}{d_0} \right)^{\alpha}. \qquad (2)$$

In Eq.(2), d_0 represents the near-field range of the transmit antenna, within which the power-law of the path-loss is invalid, while Ω_0 is the corresponding reference path-loss. The path-loss exponent is denoted as α in Eq.(2).

The wireless channels between the H-BS and the UEs obey the uncorrelated block fading [32]. The channel coefficients remains unchanged during a single transmission frame but they vary from a transmission frame to another. The downlink channel coefficient between the H-BS and U_i is represented by a $1 \times N_t$ column vector $\mathbf{h}_i$. Since the channel reciprocity is assumed, the uplink channel coefficient is thus $\mathbf{h}_i^T$, which is the transpose of $\mathbf{h}_i$.

C. DOWNLINK TRANSMISSIONS

Without loss of generality, the H-BS is assumed to transmit the modulated complex symbol x_i^D destined to the UE U_i during the downlink time-slot t_i^D. We have $\mathbb{E}[x_i^D x_i^{D*}] = 1$, where x_i^{D*} is the conjugate value of x_i^D. Considering an arbitrary time-slot t_j^D, during which the symbol x_j^D is transmitted by the H-BS, the RF signal received by U_i's antenna is expressed as

$$y_{i,j}^D = \sqrt{\frac{P_t}{\Omega_i}} \mathbf{h}_i \mathbf{w}_t x_j^D + z_0, \qquad (3)$$

for $\forall i, j = 1, \cdots, K$, where P_t is the transmit power of the H-BS and the $N_t \times 1$ vector $\mathbf{w}_t$ is the H-BS's normalised transmit beamformer, whereas z_0 is the Gaussian distributed noise having a zero mean and a variance of σ_0^2.

As illustrated in Fig.2(b), U_i only decodes its requested information during the time-slot t_i^D. At this time-slot, the received signal $y_{i,i}^D$ is split in the power domain. A fraction $\sqrt{\rho_i}$ of $y_{i,i}^D$ is exploited for information decoding, which is expressed as

$$
\begin{aligned}
y_{i,i,id}^D &= \sqrt{\rho_i} y_{i,i}^D + z_{cov} \\
&= \sqrt{\frac{\rho_i P_t}{\Omega_i}} \mathbf{h}_i \mathbf{w}_t x_i^D + \sqrt{\rho_i} z_0 + z_{cov},
\end{aligned} \tag{4}
$$

where z_{cov} is the Gaussian distributed noise incurred by the imperfect passband-to-baseband converter. The mean of z_{cov} is zero and its variance is σ_{cov}^2. As a result, the corresponding downlink throughput of U_i is formulated as

$$
\begin{aligned}
R_i^D &= t_i^D \cdot \log\left(1 + \frac{\rho_i P_t \mathbf{h}_i \mathbf{w}_t \mathbf{w}_t^* \mathbf{h}_i^*}{\Omega_i(\rho_i \sigma_0^2 + \sigma_{cov}^2)}\right) \\
&\approx t_i^D \cdot \log\left(1 + \frac{\rho_i P_t \mathbf{h}_i \mathbf{w}_t \mathbf{w}_t^* \mathbf{h}_i^*}{\Omega_i \sigma_{cov}^2}\right),
\end{aligned} \tag{5}
$$

where $\mathbf{w}_t^*$ and $\mathbf{h}_i^*$ are the conjugate transpose of the vectors $\mathbf{w}_t$ and $\mathbf{h}_i$. The approximation of Eq.(5) is obtained because the power of the antenna noise is normally far lower than that of the passband-to-baseband converter noise [33].

The RF signal $y_{i,j}^D$ received by U_i during the time-slot t_j^D for $j \neq i$ is fully exploited for energy harvesting. The received power of $y_{i,j}^D$ is $P_{i,j}^D = P_t \Omega_i^{-1} \mathbf{h}_i \mathbf{w}_t \mathbf{w}_t^* \mathbf{h}_i^*$. The energy harvested by U_i during this time-slot is thus expressed as

$$
E_{i,j}^D = \zeta t_j^D P_{i,j}^D = \zeta t_j^D P_t \Omega_i^{-1} \mathbf{h}_i \mathbf{w}_t \mathbf{w}_t^* \mathbf{h}_i^*, \tag{6}
$$

for $i \neq j$, where ζ is the RF-DC conversion efficiency. During the time-slot t_i^D, the fraction $\sqrt{1 - \rho_i}$ of the received signal $y_{i,i}^D$ is exploited by U_i for energy harvesting. Therefore, the amount of energy harvested by U_i during this time-slot is expressed as

$$
E_{i,i}^D = \zeta t_i^D (1 - \rho_i) P_t \Omega_i^{-1} \mathbf{h}_i \mathbf{w}_t \mathbf{w}_t^* \mathbf{h}_i^*. \tag{7}
$$

As a result, the total energy harvested by U_i during all the downlink time-slots $\mathbf{t}^D$ can be derived as

$$
\begin{aligned}
E_i^D &= \sum_{j=1, j \neq i}^{K} E_{i,j}^D + E_{i,i}^D \\
&= \zeta P_t \Omega_i^{-1} \mathbf{h}_i \mathbf{w}_t \mathbf{w}_t^* \mathbf{h}_i^* \left(\sum_{j=1, j \neq i}^{K} t_j^D + (1 - \rho_i) t_i^D\right) \\
&= \gamma_i \left(\sum_{j=1, j \neq i}^{K} t_j^D + (1 - \rho_i) t_i^D\right).
\end{aligned} \tag{8}
$$

where we have $\gamma_i = \zeta P_t \Omega_i^{-1} \mathbf{h}_i \mathbf{w}_t \mathbf{w}_t^* \mathbf{h}_i^*$ to simplify the expression. Note that during the downlink transmission, the H-BS adopts the identical transmit beamformer $\mathbf{w}_t$ for

all the downlink time-slots $\mathbf{t}^D$, which form a multicast beam for the SWIPT. As a result, the choice of the transmit beamformer $\mathbf{w}_t$ may satisfy the data and energy requests of the multiple UEs, which avoids the complexity of finding the optimal point-to-point transmit beamformer for every single downlink time-slot.

D. UPLINK TRANSMISSIONS

As illustrated in Fig.2(b), U_i only uploads its own data to the H-BS during the uplink time-slot t_i^U but remain silent during others. The transmit power of U_i is $P_i^U = E_i^D / t_i^U$, since all the energy harvested by U_i during the downlink transmission is now depleted for powering its own uplink transmission. As a result, the RF signals received by the H-BS's multiple antennas during the uplink time-slot t_i^U is obtained as

$$
\mathbf{y}_i^U = \sqrt{\frac{E_i^D}{t_i^U}} \mathbf{h}_i^T x_i^U + \mathbf{z}_0, \tag{9}
$$

where x_i^U having $\mathbb{E}[x_i^U x_i^{U*}]$ is the modulated complex symbol uploaded by U_i and the $N_t \times 1$ vector $\mathbf{z}_0$ represents the Gaussian distributed noise received by the antennas of the H-BS. Every element in $\mathbf{z}_0$ has a zero mean and a variance of σ_0^2. The received signal $\mathbf{y}_i^U$ is then combined by the $1 \times N_t$ receiver beamformer $\mathbf{w}_{i,r}$, which yields the signal for information decoding:

$$
\begin{aligned}
y_{i,id}^U &= \mathbf{w}_{i,r} \mathbf{y}_i^U + z_{cov} \\
&= \sqrt{\frac{E_i^D}{t_i^U}} \mathbf{w}_{i,r} \mathbf{h}_i^T x_i^U + \mathbf{w}_{i,r} \mathbf{z}_0 + z_{cov},
\end{aligned} \tag{10}
$$

where z_{cov} is the Gaussian distributed noise incurred by the imperfect passband-to-baseband converter of the H-BS. We assume that the power of the converter noise at the H-BS is equal to that of the UE. Since the maximum-ratio-combination (MRC) [34] has been proven to be the optimal receiver beamformer, the corresponding $\mathbf{w}_{i,r}$ can be expressed as

$$
\mathbf{w}_{i,r} = \sqrt{\frac{\mathbf{h}_i \mathbf{h}_i^*}{N_t}} \mathbf{h}_i. \tag{11}
$$

As a result, the uplink throughput of U_i can be formulated as

$$
\begin{aligned}
R_i^U &= t_i^U \cdot \log\left(1 + \frac{E_i^D}{t_i^U} \frac{\mathbf{w}_{i,r} \mathbf{h}_i^T \mathbf{h}_i^{T*} \mathbf{w}_{i,r}^*}{\mathbf{w}_{i,r} \mathbf{w}_{i,r}^* \sigma_0^2 + \sigma_{cov}^2}\right) \\
&\approx t_i^U \cdot \log\left(1 + \frac{E_i^D}{t_i^U} \frac{\mathbf{w}_{i,r} \mathbf{h}_i^T \mathbf{h}_i^{T*} \mathbf{w}_{i,r}^*}{\sigma_{cov}^2}\right) \\
&= t_i^U \cdot \log\left(1 + \frac{E_i^D}{t_i^U} \frac{\mathbf{h}_i(\mathbf{h}_i^* \mathbf{h}_i)(\mathbf{h}_i^* \mathbf{h}_i)^T \mathbf{h}_i^*}{N_t \sigma_{cov}^2}\right) \\
&= t_i^U \cdot \log\left(1 + \frac{E_i^D}{t_i^U} \frac{g_i}{\sigma_{cov}^2}\right)
\end{aligned} \tag{12}
$$

where E_i^D is given by Eq.(8) and the second approximation is derived by ignoring the negligibly low antenna noise

power σ_0^2. The third equality of Eq.(12) is derived by substituting Eq.(11) into Eq.(12), while the fourth equality is derived by letting $g_i = \frac{\mathbf{h}_i(\mathbf{h}_i^*\mathbf{h}_i)(\mathbf{h}_i^*\mathbf{h}_i)^T\mathbf{h}_i^*}{N_t}$.

III. UPLINK SUM-THROUGHPUT MAXIMIZATION

In this section, the time-, power- and spatial-domain resource allocation scheme is designed for maximising the UEs' uplink *sum-throughput*. The original optimisation problem is decomposed into two sub-problems, which aim for optimising the time- and power-domain resource allocation and for optimising the spatial-domain resource allocation, respectively. By invoking the SCA, an iterative algorithm is proposed for alternatively optimising this pair of sub-problems in order to obtain the optimal solution.

The uplink sum-throughput maximisation problem is then formulated as

$$(P1): \quad \max_{\mathbf{w}_t, \mathbf{t}^D, \mathbf{t}^U, \boldsymbol{\rho}} \sum_{i=1}^{K} R_i^U(\mathbf{w}_t, \mathbf{t}^D, t_i^U, \rho_i) \quad (13)$$

$$\text{s. t.} \quad R_i^D(\mathbf{w}_t, t_i^D, \rho_i) \geq D_i, \ \forall i = 1, \cdots, K, \quad (13a)$$

$$0 \leq \rho_i \leq 1, \ \forall i = 1, \cdots, K, \quad (13b)$$

$$\sum_{i=1}^{K}(t_i^D + t_i^U) \leq T_t, \quad (13c)$$

$$\text{Tr}(\mathbf{w}_t\mathbf{w}_t^*) \leq 1. \quad (13d)$$

As expressed in Eq.(13), the objective of the optimisation problem (P1) is to maximise the uplink sum-throughput of all the UEs by optimising the transmit beamformer $\mathbf{w}_t$ in the spatial-domain, by optimising the duration of the downlink time-slots $\mathbf{t}^D$ and that of the uplink time-slots $\mathbf{t}^U$ in the time-domain as well as by optimising the power splitting ratios $\boldsymbol{\rho} = \{\rho_i | i = 1, \cdots, K\}$ in the power domain. The uplink throughput R_i^U of U_i in the objective (13) is a function of $\mathbf{w}_t$, $\mathbf{t}^D, t_i^U$ and ρ_i, according to Eq.(12). The downlink throughput R_i^D of Eq.(5) is a function of $\mathbf{w}_t$, t_i^D and ρ_i, which has to be higher than U_i's downlink throughput requirement D_i, as expressed in the constraint (13a). The power splitting ratios $\boldsymbol{\rho}$ are naturally constrained by (13b). As expressed in the constraint (13c), the total duration of all the downlink and uplink time-slots should be lower than the duration of the transmission phase T_t. The constraint (13d) represents that the total power weights of the normalised transmit beamformer should be lower than a unity, where $\text{Tr}(\cdot)$ represents the trace of a matrix. By letting $\mathbf{W}_t = \mathbf{w}_t\mathbf{w}_t^*$, the constraint (13d) is equivalent to the following pair: $\text{Tr}(\mathbf{W}_t) \leq 1$ and $\text{Rank}(\mathbf{W}_t) = 1$. The rank constraint imposes difficulty in solving the problem (P1). As a result, we relax the rank constraint on the semi-definite transmit beamforming matrix $\mathbf{W}_t$, which is well known as the semi-definite relaxation (SDR). Then, instead of $\mathbf{w}_t$, we will focus on the optimisation of the transmit beamforming matrix $\mathbf{W}_t$ without any rank constraint in the spatial-domain. By solving the relaxed problem (P1), we may obtain the optimal multi-dimensional resource allocation scheme $\{\mathbf{t}^{D\dagger}, \mathbf{t}^{U\dagger}, \boldsymbol{\rho}^\dagger, \mathbf{W}_t^\dagger\}$.

Unfortunately, due to the coupled parameters $\{\mathbf{t}^D, \mathbf{t}^U, \boldsymbol{\rho}, \mathbf{W}_t\}$, (P1) is still a non-convex problem.

As a result, according to the basic principle of the SCA [35], (P1) can be decomposed into the following pair of sub-problems (P2) and (P3). Given a specific transmit beamforming matrix $\mathbf{W}_t$ satisfying $\text{Tr}(\mathbf{W}_t) \leq 1$, the sub-problem (P2) is formulated as

$$(P2): \quad \max_{\mathbf{t}^D, \mathbf{t}^U, \boldsymbol{\rho}} \sum_{i=1}^{K} R_i^U(\mathbf{t}^D, t_i^U, \rho_i | \mathbf{W}_t) \quad (14)$$

$$\text{s. t.} \quad R_i^D(t_i^D, \rho_i | \mathbf{W}_t) \geq D_i, \ \forall i = 1, \cdots, K, \quad (14a)$$

$$(13b) \text{ and } (13c). \quad$$

According to Eqs.(5) and (12), the downlink throughput R_i^D and the uplink throughput R_i^U are both functions of $\mathbf{t}^D$, $\mathbf{t}^U$ and $\boldsymbol{\rho}$. As expressed in the objective (14), given $\mathbf{W}_t$, (P2) aims for maximising the uplink sum-throughput by optimising the time- and power-domain resource allocation scheme $\{\mathbf{t}^{D\ddagger}, \mathbf{t}^{U\ddagger}, \boldsymbol{\rho}^\ddagger | \mathbf{W}_t\}$.

Given a specific time- and power-domain resource allocation scheme $\{\mathbf{t}^D, \mathbf{t}^U, \boldsymbol{\rho}\}$, the sub-problem (P3) is formulated as

$$(P3): \quad \max_{\mathbf{W}_t} \sum_{i=1}^{K} R_i^U(\mathbf{W}_t | \mathbf{t}^D, t_i^U, \rho_i) \quad (15)$$

$$\text{s. t.} \quad R_i^D(\mathbf{W}_t | t_i^D, \rho_i) \geq D_i, \ \forall i = 1, \cdots, K \quad (15a)$$

$$\text{Tr}(\mathbf{W}_t) \leq 1. \quad (15b)$$

In (P3), R_i^D and R_i^U are both convex functions of $\mathbf{W}_t$, according to Eqs.(5) and (12). As formulated in the objective (15), given $\{\mathbf{t}^D, \mathbf{t}^D, \boldsymbol{\rho}\}$, the convex optimisation (P3) aims for maximising the uplink sum-throughput by optimising the transmit beamforming matrix $\mathbf{W}_t^\ddagger$.

In the rest of this section, we will elaborate on how we jointly solve (P2) and (P3) in order to obtain the optimal resource allocation scheme $\{\mathbf{W}_t^\dagger, \mathbf{t}^{D\dagger}, \mathbf{t}^{U\dagger}, \boldsymbol{\rho}^\dagger\}$.

A. FEASIBILITY OF RESOURCE ALLOCATION.

Let us first discuss the existence of a feasible resource allocation scheme. We propose a minimisation problem of the total duration of downlink time-slots $\mathbf{t}^D$ by optimising the transmit beamforming matrix $\mathbf{W}_t$, which is formulated as

$$(P1\text{-}1): \quad \min_{\mathbf{w}_t} \sum_{i=1}^{K} \frac{D_i}{\log\left(1 + \frac{P_t\mathbf{h}_i\mathbf{w}_t\mathbf{w}_t^*\mathbf{h}_i^*}{\Omega_i\sigma_{cov}^2}\right)}, \quad (16)$$

$$\text{s. t.} \quad \text{Tr}(\mathbf{W}_t) \leq 1. \quad (16a)$$

The fractional expression of the objective (16) makes the problem (P1-1) non-convex. Since a logarithmic function is monotonously increasing with respect to its argument, taking the logarithmic operation on the objective (16) may not alter the optimality of (P1-1) but convert the non-convex objective to a convex one. As a result, the non-convex (P1-1) can be

reformulated as the following convex problem:

$$(P1\text{-}2): \quad \min_{\mathbf{W}_t} \sum_{i=1}^{K} \left\{ \log D_i \right.$$
$$\left. - \log \left[\log \left(1 + \frac{P_t \mathrm{Tr}(\mathbf{h}_i^* \mathbf{h}_i \mathbf{W}_t)}{\Omega_i \sigma_{cov}^2} \right) \right] \right\}, \quad (17)$$
$$\text{s. t. } \mathrm{Tr}(\mathbf{W}_t) \leq 1, \quad (17a)$$

where we have $\mathrm{Tr}(\mathbf{h}_i^* \mathbf{h}_i \mathbf{W}_t) = \mathbf{h}_i \mathbf{w}_t \mathbf{w}_t^* \mathbf{h}_i^*$. In order to efficiently solve (P1-2), we design an algorithm by exploiting the classic interior point method [36]. We then reformulate the constrained problem (P1-2) as the following unconstrained problem:

$$(P1\text{-}3): \quad \min_{\mathbf{W}_t} f_1(\mathbf{W}_t)$$
$$= \sum_{i=1}^{K} \left\{ \log D_i - \log \left[\log \left(1 + \frac{P_t \mathrm{Tr}(\mathbf{h}_i^* \mathbf{h}_i \mathbf{W}_t)}{\Omega_i \sigma_{cov}^2} \right) \right] \right\}$$
$$- \phi(1 - \mathrm{Tr}(\mathbf{W}_t)) - \phi(\mathrm{Det}(\mathbf{W}_t)), \quad (18)$$

where $\mathrm{Det}(\cdot)$ is the determinant operation on a matrix and $\phi(u)$ is the logarithmic barrier function [36], which is given by

$$\phi(u) = \begin{cases} \dfrac{\log(u)}{m}, & u > 0, \\ -\infty, & u \leq 0, \end{cases} \quad (19)$$

where the barrier parameter m should be higher than 0. The gradient of $f_1(\mathbf{W}_t)$ can then be derived as

$$\nabla_{\mathbf{W}_t} f_1(\mathbf{W}_t)$$
$$= \sum_{i=1}^{K} \frac{\mathbf{h}_i^* \mathbf{h}_i}{\left(\Omega_i \sigma_{cov}^2 + \mathrm{Tr}(\mathbf{h}_i^* \mathbf{h}_i \mathbf{W}_t)\right) \log \left(1 + \frac{P_t \mathrm{Tr}(\mathbf{h}_i^* \mathbf{h}_i \mathbf{W}_t)}{\Omega_i \sigma_{cov}^2} \right)}$$
$$+ \frac{1}{m} \left(\frac{\mathbf{I}}{1 - \mathrm{Tr}(\mathbf{W}_t)} - \mathbf{W}_t^{-1} \right), \quad (20)$$

where $\mathbf{I}$ is a $N_t \times N_t$ identity matrix.

When we have a specific transmit beamforming matrix $\mathbf{W}_t$, the searching direction is thus defined as $\Delta \mathbf{W}_t = \nabla_{\mathbf{W}_t} f_1(\mathbf{W}_t)$. As a result, after the n-th iteration, the transmit beamforming matrix is updated as $\mathbf{W}_t^{(n+1)} = \mathbf{W}_t^{(n)} - \theta \cdot \Delta \mathbf{W}_t$, where θ is a scalar representing the searching step. In order to guarantee the accuracy of the gradient descent method, the optimal searching step is obtained as

$$\theta = \arg \min_{\theta} f_1(\mathbf{W}_t - \theta \cdot \Delta \mathbf{W}_t). \quad (21)$$

The gradient-descent method based algorithm for solving the problem (P1-3) is thus detailed in Algorithm 1, which returns us the optimal transmit beamforming matrix $\mathbf{W}_{t,0}^{\dagger}$. Note that, the transmit beamforming matrix $\mathbf{W}_t$ in Algorithm 1 can be initialised by the equal gain beamformer $\mathbf{I}/N_t$.

If the resultant minimum total duration $T_{\min}^{D\ddagger}$ of the downlink time-slots is higher than T_t, the downlink throughput requirements $\mathbf{D} = \{D_1, \cdots, D_K\}$ cannot be satisfied. This tells us that no feasible resource allocation

---

Algorithm 1 The Gradient-Descent Method Based Algorithm for Solving Problems (P1-3), (P3-1) and (P6-2)

Input: Path loss of $\{\Omega_1, \cdots, \Omega_K\}$; Channel fading coefficients of $\{\mathbf{h}_1, \cdots, \mathbf{h}_K\}$; Transmit power of the H-BS P_t; Initial transmit beamforming matrix $\mathbf{W}_t$; Noise power of the converter σ_{cov}^2; Duration of the transmission phase T_t; Resource allocation scheme in time- and power-domain $\{\mathbf{t}^D, \mathbf{t}^U, \boldsymbol{\rho}\}$; Error tolerance ϵ.

Output: Optimal transmit beamforming matrix $\mathbf{W}_{t,0}^{\dagger}$ or $\mathbf{W}_t^{\dagger}$;

1: Obtain the searching direction gradient $\Delta \mathbf{W}_t \leftarrow \nabla_{\mathbf{W}_t} f_1(y)$ by Eq.(20), or $\Delta \mathbf{W}_t \leftarrow \nabla_{\mathbf{W}_t} f_2(y)$ by Eq.(30), or $\Delta \mathbf{W}_t \leftarrow \nabla_{\mathbf{W}_t} f_3(y)$ by Eq.(44);
2: **while** $||\Delta \mathbf{W}_t|| \leq \epsilon$ **do**
3:     Obtain the searching step θ by solving Eq.(21), or by solving Eq.(32), or by Eq.(45);
4:     Update $\mathbf{W}_t \leftarrow \mathbf{W}_t \mp \theta \Delta \mathbf{W}_t$;
5:     Obtain the searching direction gradient $\Delta \mathbf{W}_t \leftarrow \nabla_{\mathbf{W}_t} f_1(y)$ by Eq.(20), or $\Delta \mathbf{W}_t \leftarrow \nabla_{\mathbf{W}_t} f_2(y)$ by Eq.(30), or $\Delta \mathbf{W}_t \leftarrow \nabla_{\mathbf{W}_t} f_3(y)$ by Eq.(44).
6: **end while**
7: **return** $\mathbf{W}_{t,0}^{\dagger}$ or $\mathbf{W}_t^{\dagger} = \mathbf{W}_t$.

---

scheme $\{\mathbf{t}^D, \mathbf{t}^U, \boldsymbol{\rho}, \mathbf{W}_t\}$ exist for maximising the uplink sum-throughput of the UEs. Hence, the H-BS may reject the access request of some UEs in order to find a feasible resource allocation scheme.

Note that Algorithm 1 can also be exploited for solving all the optimisation problem of the transmit beamforming matrix $\mathbf{W}_t$ in this paper, which includes the problems (P1-3), (P3-1) and (P6-2).

B. RESOURCE ALLOCATION IN TIME- AND POWER-DOMAIN

The sub-problem (P2) is still non-convex, due to the coupled parameters $\mathbf{t}^D$ and $\boldsymbol{\rho}$ induced by Eq.(8). By defining $\boldsymbol{\mu} = \{\mu_i = t_i^D(1 - \rho_i)|, i = 1, \cdots, K\}$, (P2) is equivalently transformed to the following convex optimisation problem (P2-1), which is formulated as

$$(P2\text{-}1): \quad \max_{\mathbf{t}^D, \mathbf{t}^U, \boldsymbol{\mu}} \sum_{i=1}^{K} R_i^U(\mathbf{t}^D, t_i^U, \mu_i | \mathbf{W}_t) \quad (22)$$
$$\text{s. t. } R_i^D(t_i^D, \mu_i | \mathbf{W}_t) \geq D_i, \ \forall i = 1, \cdots, K, \quad (22a)$$
$$0 \leq \mu_i \leq t_i^D, \ \forall i = 1, \cdots, K, \text{ and (13c)}. \quad (22b)$$

By exploiting the classic Lagrange multiplier method, the corresponding Lagrange function of (P2-1) is derived as

$$\mathcal{L}(\mathbf{t}^D, \mathbf{t}^U, \boldsymbol{\mu}, \lambda, \boldsymbol{\xi})$$
$$= \sum_{i=1}^{K} R_i^U(\mathbf{t}^D, t_i^U, \mu_i | \mathbf{W}_t) + \lambda \left[T_c - \sum_{i=1}^{K} (t_i^D + t_i^U) \right]$$
$$+ \sum_{i=1}^{K} \xi_i [R_i^D(t_i^D, \mu_i | \mathbf{W}_t) - D_i], \quad (23)$$

where λ and $\boldsymbol{\xi} = \{\xi_i | i = 1, \cdots, K\}$ are the Lagrange multipliers for the constraints (13c) and (22a), respectively. The optimal solution $\{\mathbf{t}^{D\ddagger}, \mathbf{t}^{U\ddagger}, \boldsymbol{\mu}^{\ddagger}\}$ of (P2-1) have to satisfy the following Karush-Kuhn-Tucker (KKT) conditions:

$$
\begin{cases}
\log(1 + p_i) - \dfrac{p_i}{1 + p_i} = \lambda \\
\dfrac{\sum_{j=1}^{K} g_j \gamma_j}{(1 + p_i)\sigma_{cov}^2} + \xi_i [\log(1 + q_i) - \dfrac{q_i}{1 + q_i}] = \lambda \\
\dfrac{g_i}{1 + y_i} = \xi_i \dfrac{1}{1 + q_i} \\
\sum_{i=1}^{K} (t_i^D + t_i^U) = T_t, \\
t_i^D \log(1 + q_i) = D_i,
\end{cases}
\tag{24}
$$

for $\forall i = 1, \cdots, K$, where we have $p_i = \frac{\gamma_i g_i \sum_{j=1}^{K} t_j^D - \mu_i}{\sigma_{cov}^2}$ and $q_i = \frac{\mu_i \gamma_i}{t_i^D \sigma_{cov}^2}$. Specifically, γ_i and g_i are defined in Eqs.(8) and (12), respectively. Given a specific value of λ, the optimal solution can be derived as

$$
\begin{cases}
t_i^{D\ddagger} = \dfrac{D_i}{\log(1 + q_i^{\ddagger})}, \\
t_i^{U\ddagger} = h_i \gamma_i \dfrac{\sum_{j=1}^{K} t_j^{D\ddagger} - \mu_i^{\ddagger}}{p_i^{\ddagger} \sigma_{cov}^2}, \\
\mu_i^{\ddagger} = \dfrac{q_i^{\ddagger} \sigma_{cov}^2}{\gamma_i t_i^{D\ddagger}},
\end{cases}
\tag{25}
$$

where $p_i^{\ddagger}$ and $q_i^{\ddagger}$ can be obtained by solving the following system of equations:

$$
\log(1 + p_i) - \frac{p_i}{1 + p_i} = \lambda,
\tag{26}
$$

$$
(1 + q_i)\log(1 + q_i) - q_i = \frac{\lambda(1 + p_i) - \sum_{j=1}^{K} \frac{g_j \gamma_j}{\sigma^2}}{g_i},
\tag{27}
$$

The left-hand side of Eq.(26) is a monotonously increasing function of p_i, while the left-hand side of Eq.(27) is a monotonously increasing function of q_i. Observe from their respective right-hand side that both p_i and q_i monotonously increase as we increase λ. Note that q_i is positive, which determines that the right-hand side of Eq.(27) should be higher than zero. Furthermore, increasing λ leads to the increment of the right-hand side of Eq.(27). Therefore, if the right-hand side of Eq.(27) is lower than zero, we should increase λ. The details of the binary search based algorithm is provided in Algorithm 2. Note that similar methodology has been used for obtaining the optimal time-domain resource allocation scheme for maximising the sum-throughput in our previous work [28]. However, the binary searching based Algorithm 2 proposed in this paper substantially reduces the complexity of the time- and power-domain resource allocation, when compared to the algorithm proposed in [28].

C. RESOURCE ALLOCATION IN SPATIAL-DOMAIN
After relaxing the rank constraint, the sub-problem (P3) is transformed into a convex optimisation problem.

Algorithm 2 A Binary Search Based Algorithm for Solving (P2-1)

Input: Path loss of $\{\Omega_1, \cdots, \Omega_K\}$; Channel fading coefficients of $\{\mathbf{h}_1, \cdots, \mathbf{h}_K\}$; Transmit power of the H-BS P_t; Transmit beamforming matrix $\mathbf{W}_t$; Noise power of the converter σ_{cov}^2; Duration of the transmission phase T_t; Error tolerance ϵ.

Output: Optimal resource allocation scheme $\{\mathbf{t}^{D\ddagger}, \mathbf{t}^{U\ddagger}, \boldsymbol{\rho}^{\ddagger}\}$ in time- and power-domain.

1: Initialise $\lambda_{\min} \leftarrow 0$, $\lambda_{\max} \leftarrow$ A sufficiently large value;
2: **while** $\lambda_{\max} - \lambda_{\min} > \epsilon$ **do**
3:      Update $\lambda_{mid} \leftarrow \frac{1}{2}(\lambda_{\max} + \lambda_{\min})$;
4:      Obtain $\mathbf{p}^{\ddagger} \leftarrow \{p_1^{\ddagger}, \cdots, p_K^{\ddagger}\}$ by substituting λ_{mid} into Eq.(26);
5:      **if** $\lambda_{mid}(1 + p_i^{\ddagger}) - \sum_{j=1}^{K} \frac{g_j \gamma_j}{\sigma_{cov}^2} > 0, \forall i$ **then**
6:          Obtain $\mathbf{q}^{\ddagger} \leftarrow \{q_1^{\ddagger}, \cdots, q_K^{\ddagger}\}$ by substituting λ_{mid} and $\mathbf{p}^{\ddagger}$ into Eq.(27);
7:          Obtain $\{\mathbf{t}^{D\ddagger}, \mathbf{t}^{U\ddagger}, \boldsymbol{\mu}^{\ddagger}\}$ by substituting $\mathbf{p}^{\ddagger}$ and $\mathbf{q}^{\ddagger}$ into Eq.(25)
8:          **if** $\sum_{i=1}^{K} t_i^{D\ddagger} + t_i^{U\ddagger} \leq T_t$ **then**
9:              Update $\lambda_{\max} \leftarrow \lambda_{mid}$;
10:          **else**
11:              Update $\lambda_{\min} \leftarrow \lambda_{mid}$;
12:          **end if**
13:      **else**
14:          Update $\lambda_{\min} \leftarrow \lambda_{mid}$;
15:      **end if**
16: **end while**
17: Obtain $\boldsymbol{\rho}^{\ddagger} \leftarrow \{\rho_i^{\ddagger} = \frac{\mu_i^{\ddagger}}{t_i^{D\ddagger}} | i = 1, \cdots, K\}$;
18: **return** $\{\mathbf{t}^{D\ddagger}, \mathbf{t}^{U\ddagger}, \boldsymbol{\rho}^{\ddagger}\}$

Similarly to (P1-1), we also exploit the interior point method for efficiently solving this convex problem. Then, the original constrained problem (P3) is reformulated as the following unconstrained problem:

$$
\text{(P3-1):} \quad \max_{\mathbf{W}_t} f_2(\mathbf{W}_t)
$$

$$
= \sum_{i=1}^{K} \left[R_i^U(\mathbf{W}_t | \mathbf{t}^D, t_i^U, \boldsymbol{\rho}) + \phi(\text{Tr}(\mathbf{h}_i^* \mathbf{h}_i \mathbf{W}_t) - a_i) \right]
$$

$$
+ \phi(1 - Tr(\mathbf{W}_t)) + \phi(\det(\mathbf{W}_t)),
\tag{28}
$$

where $\phi(u)$ is the logarithmic barrier function given by Eq.(19). Furthermore, the parameter a_i in (P3-1) is given by

$$
a_i = \frac{\sigma_{cov}^2}{\rho_i \Omega_i} (e^{\frac{D_i}{t_i^D}} - 1),
\tag{29}
$$

for $\forall i$. The unconstrained problem (P3-1) can thus be solved by exploiting the gradient descent method. Given a feasible $\mathbf{W}_t$, the gradient of $f_2(\mathbf{W}_t)$ can be

derived as

$$
\begin{aligned}
&\nabla_{\mathbf{W}_t} f_2(\mathbf{W}_t) \\
&= \frac{1}{m} \left(\sum_{i=1}^{K} \frac{\mathbf{h}_i^* \mathbf{h}_i}{\mathrm{Tr}(\mathbf{h}_i^* \mathbf{h}_i \mathbf{W}_t) - a_i} - \frac{\mathbf{I}}{1 - \mathrm{Tr}(\mathbf{W}_t)} + \mathbf{W}_t^{-1} \right) \\
&\quad + \sum_{i=1}^{K} \frac{t_i^U b_i \mathbf{h}_i^* \mathbf{h}_i}{1 + b_i \mathrm{Tr}(\mathbf{h}_i^* \mathbf{h}_i \mathbf{W}_t)},
\end{aligned} \tag{30}
$$

where $\mathbf{I}$ is an $N_t \times N_t$ identity matrix and the parameter b_i is expressed as

$$
b_i = \frac{\Omega_i g_i (\sum_{j=1}^{K} t_j^D - t_i^D \rho_i)}{t_i^U \sigma_{cov}^2}, \tag{31}
$$

The optimal searching step is obtained as

$$
\theta = \arg \min_\theta f_2(\mathbf{W}_t + \theta \cdot \Delta \mathbf{W}_t), \tag{32}
$$

where $\Delta \mathbf{W}_t = \nabla_{\mathbf{W}_t} f_2(\mathbf{W}_t)$ is the searching direction. As a result, after the n-th iteration, the transmit beamforming matrix is updated as $\mathbf{W}_t^{(n+1)} = \mathbf{W}_t^{(n)} + \theta \cdot \Delta \mathbf{W}_t$. Therefore, the optimal transmit beamforming matrix $\mathbf{W}_t^{\ddagger}$ in the spatial domain can be then obtained by exploiting Algorithm 1.

D. SCA BASED ALGORITHM

The optimal resource allocation scheme $\{\mathbf{t}^{D\dagger}, \mathbf{t}^{U\dagger}, \boldsymbol{\rho}^\dagger, \mathbf{W}_t^\dagger\}$ to (P1) can then be obtained by alternatively solving (P2-1) and (P3-1), which is detailed in Algorithm 3. Note that the existence of a feasible resource allocation scheme to (P1) is validated by solving (P1-2) in Algorithm 1. This may substantially increase the robustness and reduce the complexity of the SCA based Algorithm 3.

IV. UPLINK FAIR-THROUGHPUT MAXIMIZATION

The UEs in the vicinity of the BS have good uplink channels for satisfying their data uploading requirements. The improvement of their uplink throughput is substantial, when more resources are allocated to these UEs. However, the poor channels connecting the distant UEs to the BS largely restricts their uplink throughputs. Even if more resources are allocated to these UEs, the improvement of their uplink throughput is limited. As a result, in order to maximise the uplink sum-throughput, the BS may allocate more resources to the UEs in its vicinity, since it may results in substantial growth of the sum-throughput, while the data uploading requests of the distant UEs may be largely ignored by the BS. This is the classic "near-far effect" of the multi-user WIT system.

In the WPCN, the uplink transmission of the UEs is constrained by the energy harvested from the downlink RF signals transmitted by the H-BS, as expressed in Eq.(12). The UEs in the vicinity of the H-BS may harvest more energy from the downlinks than their distant counterparts, which further increase the gap between their uploading capabilities. Therefore, the H-BS is more willing to allocate resources to its nearby UEs, which results in the "doubly near-far effect" [12].

Algorithm 3 SCA Based Algorithm for Solving (P1)

Input: Path loss of $\{\Omega_1, \cdots, \Omega_K\}$; Channel fading coefficients of $\{\mathbf{h}_1, \cdots, \mathbf{h}_K\}$; Transmit power of the H-BS P_t; Noise power of the converter σ_{cov}^2; Duration of the transmission phase T_t; Error tolerance ϵ.

Output: Optimal resource allocation scheme $\{\mathbf{t}^{D\dagger}, \mathbf{t}^{U\dagger}, \boldsymbol{\rho}^\dagger, \mathbf{W}_t^\dagger\}$ in time- power- and spatial-domain; Maximum uplink sum-throughput $R_{\mathrm{sum}}^\dagger$.

1: Initialise the transmit beamforming matrix $\mathbf{W}_t \leftarrow \mathbf{I}/N_t$ in Algorithm 1;
2: Obtain a feasible transmit beamforming matrix $\mathbf{W}_{t,0}^{\ddagger}$ and the resultant minimum total duration $T_{\min}^{D\ddagger}$ of the downlink time-slots by solving (P1-3) based on Algorithm 1;
3: **if** $T_{\min}^{D\ddagger} < T_t$ **then**
4:     Initialise an uplink sum-throughput recorder $R_{\mathrm{sum},0} \leftarrow 0$;
5:     Initialise another uplink sum-throughput recorder $R_{\mathrm{sum},1} \leftarrow 2\epsilon$;
6:     Initialise the transmit beamforming matrix $\mathbf{W}_t \leftarrow \mathbf{W}_{t,0}^{\ddagger}$ in Algorithm 2 for solving (P2-1);
7:     Initialise the transmit beamforming matrix $\mathbf{W}_t \leftarrow \mathbf{W}_{t,0}^{\ddagger}$ in Algorithm 1 for solving (P3-1);
8:     **while** $R_{\mathrm{sum},1} - R_{\mathrm{sum},0} > \epsilon$ **do**
9:        Update $R_{\mathrm{sum},0} \leftarrow R_{\mathrm{sum},1}$;
10:       Obtain the optimal solution $\{\mathbf{t}^{D\ddagger}, \mathbf{t}^{U\ddagger}, \boldsymbol{\rho}^\ddagger\}$ to (P2-1) based on Algorithm 2;
11:       Update $\{\mathbf{t}^D, \mathbf{t}^U, \boldsymbol{\rho}\} \leftarrow \{\mathbf{t}^{D\ddagger}, \mathbf{t}^{U\ddagger}, \boldsymbol{\rho}^\ddagger\}$ in Algorithm 1 for solving (P3-1);
12:       Obtain the optimal solution $\mathbf{W}_t^{\ddagger}$ to (P3-1) and the resultant uplink sum-throughput $R_{\mathrm{sum}}^{\ddagger}$ based on Algorithm 1;
13:       Update $R_{\mathrm{sum},1} \leftarrow R_{\mathrm{sum}}^{\ddagger}$;
14:       Update $\mathbf{W}_t \leftarrow \mathbf{W}_t^{\ddagger}$ in Algorithm 1 for solving (P3-1) and in Algorithm 2 for solving (P2-1);
15:     **end while**
16:     Update $\{\mathbf{t}^{D\dagger}, \mathbf{t}^{U\dagger}, \boldsymbol{\rho}^\dagger, \mathbf{W}_t^\dagger\} \leftarrow \{\mathbf{t}^{D\ddagger}, \mathbf{t}^{U\ddagger}, \boldsymbol{\rho}^\ddagger, \mathbf{W}_t^{\ddagger}\}$, $R_{\mathrm{sum}}^\dagger \leftarrow R_{\mathrm{sum}}^{\ddagger}$;
17: **else**
18:     No feasible resource allocation scheme.
19: **end if**
20: **return** $\{\mathbf{t}^{D\dagger}, \mathbf{t}^{U\dagger}, \boldsymbol{\rho}^\dagger, \mathbf{W}_t^\dagger\}$ and $R_{\mathrm{sum}}^\dagger$.

In order to overcome the unfairness incurred by the "doubly near-far effect", we aim for maximising the uplink *fair-throughput* in our IDEN, which is defined as the minimum uplink throughput among the UEs. As a result, the uplink fair-throughput maximisation problem is formulated as

$$
(\text{P4}): \quad \max_{\mathbf{t}^D, \mathbf{t}^U, \boldsymbol{\rho}, \mathbf{w}_t} R_{\mathrm{fair}} \tag{33}
$$

$$
\text{s. t. } R_i^U(\mathbf{w}_t, \mathbf{t}^D, t_i^U, \rho_i) \geq R_{\mathrm{fair}}, \forall i = 1, \cdots, K, \tag{33a}
$$

$$R_i^D(\mathbf{w}_t, t_i^D, \rho_i) \geq D_i, \forall i = 1, \cdots, K, \quad (33\text{b})$$

$$0 \leq \rho_i \leq 1, \forall i = 1, \cdots, K, \quad (33\text{c})$$

$$\sum_{i=1}^{K} (t_i^D + t_i^U) \leq T, \quad (33\text{d})$$

$$\text{Tr}(\mathbf{w}_t \mathbf{w}_t^*) \leq 1. \quad (33\text{e})$$

As expressed in the objective (33), (P4) aims for maximising the uplink fair-throughput R_{fair} by optimising the downlink time-slots $\mathbf{t}^D$, the uplink time-slots $\mathbf{t}^U$ and the power splitting ratios $\boldsymbol{\rho}$ of the UEs as well as the transmit beamformer $\mathbf{w}_t$ of the H-BS. The constraint (33a) defines the uplink fair-throughput R_{fair}, which is not higher than the uplink throughput of every UE. Other constraints are the same as our uplink sum-throughput maximisation problem (P1). Furthermore, based on the SDR method, we also relax the inherent rank constraint of (33e) by letting $\mathbf{W}_t = \mathbf{w}_t \mathbf{w}_t^*$ and by substituting (33e) with $\text{Tr}(\mathbf{W}_t) \leq 1$.

Unfortunately, the relaxed problem (P4) is still non-convex, due to the coupled parameters $\{\mathbf{t}^D, \mathbf{t}^U, \boldsymbol{\rho}, \mathbf{W}_t\}$. By exploiting the SCA method, the relaxed problem (P4) can be decomposed into the following pair of sub-problems. Given a feasible transmit beamforming matrix $\mathbf{W}_t$ satisfying $\text{Tr}(\mathbf{W}_t) \leq 1$, the first sub-problem aims for maximising the uplink fair-throughput by finding the optimal resource allocation scheme $\{\mathbf{t}^{D\ddagger}, \mathbf{t}^{U\ddagger}, \boldsymbol{\rho}^{\ddagger}|\mathbf{W}_t\}$ in the time- and power-domain, which is formulated as

$$(\text{P5}): \quad \max_{\mathbf{t}^D, \mathbf{t}^U, \boldsymbol{\rho}} R_{\text{fair}} \quad (34)$$

$$\text{s. t. } R_i^U(\mathbf{t}^D, t_i^U, \rho_i|\mathbf{W}_t) \geq R_{\text{fair}}, \forall i = 1, \cdots, K, \quad (34\text{a})$$

$$R_i^D(t_i^D, \rho_i|\mathbf{W}_t) \geq D_i, \forall i = 1, \cdots, K, \quad (34\text{b})$$

$$(33\text{c}) \text{ and } (33\text{d}).$$

Given a feasible resource allocation scheme $\{\mathbf{t}^D, \mathbf{t}^U, \boldsymbol{\rho}\}$ in the time- and power-domain satisfying the constraints (33c) and (33d), the second sub-problem aims for maximising the uplink fair-throughput by finding the optimal transmit beamforming matrix $\{\mathbf{W}_t^{\ddagger}|\mathbf{t}^D, \mathbf{t}^U, \boldsymbol{\rho}\}$ in the spatial-domain, which is formulated as

$$(\text{P6}): \quad \max_{\mathbf{W}_t} R_{\text{fair}} \quad (35)$$

$$\text{s. t. } R_i^U(\mathbf{W}_t|\mathbf{t}^D, t_i^U, \rho_i) \geq R_{\text{fair}}, \forall i = 1, \cdots, K, \quad (35\text{a})$$

$$R_i^D(\mathbf{W}_t|t_i^D, \rho_i) \geq D_i, \forall i = 1, \cdots, K, \quad (35\text{b})$$

$$\text{Tr}(\mathbf{W}_t) \leq 1. \quad (35\text{c})$$

Moreover, the existence of the optimal resource allocation scheme for maximising the uplink fair-throughput R_{fair} can also be validated by exploiting the methodology introduced in Section III-A. The resultant transmit beamforming matrix $\mathbf{W}_{t,0}^{\ddagger}$ can also be relied upon for initialising the iterative algorithm for solving (P4), which will be detailed in Section IV-C.

In the rest of this section, we will elaborate on how we jointly solve (P5) and (P6) in order to obtain the optimal resource allocation scheme $\{\mathbf{t}^{D\dagger}, \mathbf{t}^{U\dagger}, \boldsymbol{\rho}^{\dagger}, \mathbf{W}_t^{\dagger}\}$.

A. RESOURCE ALLOCATION IN TIME- AND POWER-DOMAIN

The sub-problem (P5) is still non-convex, due to the coupled parameters $\mathbf{t}^D$ and $\boldsymbol{\rho}$. We then introduce a set of new parameters $\boldsymbol{\mu} = \{\mu_i = t_i^D(1 - \rho_i)|i = 1, \cdots, K\}$ and reformulate (P5) as

$$(\text{P5-1}): \quad \max_{\mathbf{t}^D, \mathbf{t}^U, \boldsymbol{\mu}} R_{\text{fair}} \quad (36)$$

$$\text{s. t. } R_i^U(\mathbf{t}^D, t_i^U, \mu_i|\mathbf{W}_t) \geq R_{\text{fair}}, \forall i = 1, \cdots, K, \quad (36\text{a})$$

$$R_i^D(t_i^D, \mu_i|\mathbf{W}_t) \geq D_i, \forall i = 1, \cdots, K, \quad (36\text{b})$$

$$0 \leq \mu_i \leq t_i^D, \forall i = 1, \cdots, K, \quad (36\text{c})$$

$$\sum_{i=1}^{K} (t_i^D + t_i^U) \leq T_t. \quad (36\text{d})$$

Since both the objective (36) and the constraints (36a)-(36d) are either convex or affine with respect to $\{\mathbf{t}^D, \mathbf{t}^U, \boldsymbol{\mu}\}$, (P5-1) is a convex optimisation problem. Note that the downlink throughput $R_i^D(t_i^D, \mu_i|\mathbf{W}_t)$ is a monotonously increasing function of t_i^D, while the uplink throughput $R_i^U(\mathbf{t}^D, t_i^U, \mu_i|\mathbf{W}_t)$ is also a monotonously increasing function of $\mathbf{t}_D$ and t_i^U. As a result, increasing the duration of the actual transmission phase $T_t' = \sum_{i=1}^{K} (t_i^D + t_i^U)$ may increase the fair throughput R_{fair}. In order to reduce the complexity of directly solving (P5-1), given a specific R_{fair}, we formulate the following convex optimisation problem:

$$(\text{P5-2}): \quad \min_{\mathbf{t}^D, \mathbf{t}^U, \boldsymbol{\mu}} T_t' = \sum_{i=1}^{K} (t_i^D + t_i^U), \quad (37)$$

$$\text{s. t. } (36\text{a}), (36\text{b}) \text{ and } (36\text{c}).$$

If the resultant minimum duration of the actual transmission phase $T_{t,\min}'$ is higher than T_t, the current fair-throughput R_{fair} is not feasible and it has to be reduced. By contrast, if we have $T_{t,\min}' < T_t$, the current fair-throughput R_{fair} is feasible but it has to be increased in order to achieve its maximum. Let us now focus on the details of maximising R_{fair}.

By exploiting the Lagrange multiplier method, the Lagrange function of (P5-2) can be formulated as

$$\mathcal{L}(\mathbf{t}^D, \mathbf{t}^U, \boldsymbol{\mu}, \boldsymbol{\lambda}, \boldsymbol{\xi})$$
$$= \sum_{i=1}^{K} (t_i^D + t_i^U) + \sum_{i=1}^{K} \lambda_i [R_{\text{fair}} - R_i^U(\mathbf{t}^D, t_i^U, \mu_i|\mathbf{W}_t)]$$
$$+ \sum_{i=1}^{K} \xi_i [D_i - R_i^D(t_i^D, \mu_i|\mathbf{W}_t)], \quad (38)$$

where $\boldsymbol{\lambda} = \{\lambda_i|i = 1, \cdots, K\}$ and $\boldsymbol{\xi} = \{\xi_i|i = 1, \cdots, K\}$ are the Lagrange multipliers correspond to the constraints (36a) and (36b). Given a specific range of $\boldsymbol{\lambda}$, the optimal solution $\{\mathbf{t}^{D'}, \mathbf{t}^{U'}, \boldsymbol{\mu}'\}$ of (P5-2) has to satisfy the same KKT conditions given by Eq.(24) and thus they can be expressed as Eq.(25).

However, the parameters p_i and q_i have different relationships with $\boldsymbol{\lambda}$, which are expressed as

$$\log(1 + p_i) - \frac{p_i}{1 + p_i} = \frac{1}{\lambda_i}, \tag{39}$$

$$(1 + q_i)\log(1 + q_i) - q_i = \frac{1 + p_i}{\lambda_i g_i} - \frac{\sum_{j \neq i} \lambda_j \gamma_j g_j}{\lambda_i g_i}. \tag{40}$$

Therefore, the optimal pair of $p_i^{\ddagger}$ and $q_i^{\ddagger}$ can be derived by solving Eqs.(39) and (40). Similar to Eqs.(26) and (27), the parameters p_i and q_i are also monotonously increasing with respect to the corresponding λ_i. As a result, the optimal pair $\{p_i^{\ddagger}, q_i^{\ddagger}\}$ can be obtained by invoking the classic bisection method on Eqs.(39) and (40), respectively.

Furthermore, the sub-gradient of the Lagrange function $\mathcal{L}(\mathbf{t}^{D\ddagger}, \mathbf{t}^{U\ddagger}, \boldsymbol{\mu}^{\ddagger}, \boldsymbol{\lambda}, \boldsymbol{\xi})$ with respect to $\boldsymbol{\lambda}$ is denoted as $\boldsymbol{\delta} = \{\delta_i | i = 1, \cdots, K\}$, whose i-th element is expressed as

$$\delta_i = \frac{\partial \mathcal{L}}{\partial \lambda_i} = t_i^{U\ddagger} \log(1 + p_i^{\ddagger}) - R_{\text{fair}}. \tag{41}$$

After the n-th iteration, the Lagrange multiplier set is updated as $\boldsymbol{\lambda}^{(n+1)} = \boldsymbol{\lambda}^{(n)} - \Delta_{\lambda} \boldsymbol{\delta}$, where Δ_{λ} is the searching step. The iteration for obtaining the optimal Lagrange multiplier set $\boldsymbol{\lambda}^{\ddagger}$ completes until we have $|\boldsymbol{\delta}| \leq \epsilon_{\delta}$, where ϵ_{δ} represents the absolute error tolerance on the sub-gradient.

We firstly initialise R_{fair} of (P5-2) with an arbitrary value. After solving (P5-2), we obtain the minimum duration of the transmission phase $T'_{\min,t}$. If we have $T'_{\min,t} < T_t$, we have to increase R_{fair} and solve (P5-2) again. If we have $T'_{\min,t} > T_t$, we have to reduce R_{fair} and solve (P5-2) again. The binary searching based algorithm is exploited for finding the optimal fair-throughput $R_{\text{fair}}^{\ddagger}$. The details of the algorithm for solving (P5-1) is provided in Algorithm 4. Note that similar methodology has been used for obtaining the optimal time-domain resource allocation scheme for maximising the fair-throughput in our previous work [28]. However, the binary searching based Algorithm 4 proposed in this paper substantially reduces the complexity of the time- and power-domain resource allocation, when compared to the algorithm proposed in [28].

B. RESOURCE ALLOCATION IN SPATIAL-DOMAIN

Given a specific resource allocation scheme $\{\mathbf{t}^D, \mathbf{t}^U, \boldsymbol{\rho}\}$, the fair-throughput maximisation problem (35) is convex with respect to the transmit beamforming matrix $\mathbf{W}_t$, after the SDR. Note that the uplink throughput $R_i^U(\mathbf{W}_t | \mathbf{t}^D, t_i^U, \boldsymbol{\rho})$ is a monotonously increasing function of $\text{Tr}(\mathbf{W}_t)$ and so is the downlink throughput $R_i^D(\mathbf{W}_t | t_i^D, \rho_i)$. As a result, increasing the normalised power weights $\text{Tr}(\mathbf{W}_t)$ of the transmit antennas is capable of increasing the uplink fair-throughput R_{fair}. Similarly to the formulation of (P5-2), given a specific R_{fair}, the following convex optimisation problem is formulated:

$$\text{(P6-1):} \quad \min_{\mathbf{W}_t} P'_{t,norm} = \text{Tr}(\mathbf{W}_t) \tag{42}$$

$$\text{s. t.} \quad \text{(35a) and (35b)}$$

The problem (P6-1) can be solved by invoking the interior-point method, as we have done for solving (P1-2) and (P3-1).

Algorithm 4 The Binary Searching Based Algorithm for Solving (P5-1)

Input: Path loss of $\{\Omega_1, \cdots, \Omega_K\}$; Channel fading coefficients of $\{\mathbf{h}_1, \cdots, \mathbf{h}_K\}$; Transmit power of the H-BS P_t; Feasible Transmit beamforming matrix $\mathbf{W}_t$; Noise power of the converter σ_{cov}^2; Duration of the transmission phase T_t; Searching step for the Lagrange multipliers Δ_{λ}; Error tolerance ϵ_{δ} and ϵ_r.

Output: Optimal resource allocation scheme $\{\mathbf{t}^{D\ddagger}, \mathbf{t}^{U\ddagger}, \boldsymbol{\rho}^{\ddagger}\}$ in time- and power-domain; Maximum fair-throughput $R_{\text{fair}}^{\ddagger}$.

1: Initialize $R_{\min} \leftarrow 0$ and $R_{\max} \leftarrow$ A sufficiently high value;
2: **while** $R_{\max} - R_{\min} > \epsilon_r$ **do**
3:     Initialise the fair throughput $R_{\text{fair}} \leftarrow \frac{R_{\max} + R_{\min}}{2}$;
4:     Initialize $\boldsymbol{\lambda} \leftarrow$ An arbitrary vector;
5:     Obtain $\{p_i^{\ddagger} | i = 1, \cdots, K\}$ and $\{q_i^{\dagger} | i = 1, \cdots, K\}$ by solving Eqs.(39) and (40) with the aid of the bisection method;
6:     Obtain $\{\mathbf{t}^{D\ddagger}, \mathbf{t}^{U\ddagger}, \boldsymbol{\rho}^{\ddagger}\}$ by Eq.(25);
7:     Obtain the sub-gradient $\boldsymbol{\delta} = \{\delta_i | i = 1, \cdots, K\}$ of the Lagrange function $\mathcal{L}$ by Eq.(41);
8:     **while** $|\boldsymbol{\delta}| > \epsilon_{\delta}$ **do**
9:         Update $\boldsymbol{\lambda} \leftarrow \boldsymbol{\lambda} - \Delta_{\lambda} \boldsymbol{\delta}$;
10:        Update $\{p_i^{\ddagger} | i = 1, \cdots, K\}$ and $\{q_i^{\dagger} | i = 1, \cdots, K\}$ by solving Eqs.(39) and (40);
11:        Update $\{\mathbf{t}^{D\ddagger}, \mathbf{t}^{U\ddagger}, \boldsymbol{\rho}^{\ddagger}\}$ by Eq.(25);
12:        Update the sub-gradient $\boldsymbol{\delta} = \{\delta_i | i = 1, \cdots, K\}$ of the Lagrange function $\mathcal{L}$ by Eq.(41);
13:     **end while**
14:     Obtain $T'_{\min,t} \leftarrow \sum_{i=1} K(t_i^{D\ddagger} + t_i^{U\ddagger})$;
15:     **if** $T'_{\min,t} \leq T_t$ **then**
16:        $R_{\max} \leftarrow R_{\text{fair}}$;
17:     **else**
18:        $R_{\min} \leftarrow R_{\text{fair}}$;
19:     **end if**
20: **end while**
21: Obtain $\boldsymbol{\rho}^{\ddagger} \leftarrow \{\rho_i^{\ddagger} = \frac{\mu_i^{\ddagger}}{t_i^{D\ddagger}} | i = 1, \cdots, K\}$;
22: **return** $\{\mathbf{t}^{D\ddagger}, \mathbf{t}^{U\ddagger}, \boldsymbol{\rho}^{\ddagger}\}$ and $R_{\text{fair}}^{\ddagger}$.

We then transform the original constrained problem (P6-1) to the following unconstrained problem (P6-2):

$$\text{(P6-2):} \quad \min_{\mathbf{W}_t} f_3(\mathbf{W}_t)$$

$$= \text{Tr}(\mathbf{W}_t) - \phi(\text{Det}(\mathbf{W}_t)) - \sum_{i=1}^{K} \phi\left(\text{Tr}(\mathbf{h}_i^* \mathbf{h}_i \mathbf{W}_t) - a_i\right)$$

$$- \sum_{i=1}^{K} \phi\left(\text{Tr}(\mathbf{h}_i^* \mathbf{h}_i \mathbf{W}_t) - c_i\right). \tag{43}$$

In Eq.(43), we have $c_i = (e^{\frac{R_{\text{fair}}}{t_i^U}} - 1)b_i$ and b_i has been defined in Eq.(31). The unconstrained problem (P6-2) can thus be

---

Algorithm 5 The Binary Searching Based Method for Solving (P6)

Input: Path loss of $\{\Omega_1, \cdots, \Omega_K\}$; Channel fading coefficients of $\{\mathbf{h}_1, \cdots, \mathbf{h}_K\}$; Transmit power of the H-BS P_t; Noise power of the converter σ^2_{cov}; Duration of the transmission phase T_t; Environment settings; Feasible Transmit beamforming matrix $\mathbf{W}_t$; Resource allocation scheme $\{\mathbf{t}^D, \mathbf{t}^{U\ddagger}, \boldsymbol{\rho}^{\ddagger}\}$ in time- and power-domain Error tolerance ϵ.

Output: Optimal transmit beamforming matrix $\mathbf{W}_t^{\ddagger}$; Maximum fair-throughput $R_{\text{fair}}^{\ddagger}$.

1: Initialise $R_{\min} \leftarrow 0$ and $R_{\max} \leftarrow$ a sufficiently high value;
2: Initialise $\mathbf{W}_t^{\ddagger} \leftarrow \mathbf{W}_t$;
3: **while** $R_{\max} - R_{\min} > \epsilon$ **do**
4:      Update $R_{\text{fair}}^{\ddagger} \leftarrow \frac{R_{\max} + R_{\min}}{2}$.
5:      Update $\mathbf{W}_t^{\ddagger}$ by solving (P6-2) with the aid of Algorithm 1;
6:      **if** $\text{Tr}(\mathbf{W}_t^{\ddagger}) > 1$ **then**
7:          Update $R_{\max} \leftarrow R_{\text{fair}}$
8:      **else**
9:          Update $R_{\min} \leftarrow R_{\text{fair}}$
10:      **end if**
11: **end while**
12: **return** $\mathbf{W}_t^{\ddagger}$ and $R_{\text{fair}}^{\ddagger}$.

---

solved by exploiting the gradient descent method. Given a feasible $\mathbf{W}_t$, the gradient of $f_3(\mathbf{W}_t)$ can be derived as

$$\nabla_{\mathbf{W}_t} f_3(\mathbf{W}_t) = \mathbf{I} - \frac{1}{m}\left[\mathbf{W}_t + \sum_{i=1}^{K}\left(\frac{\mathbf{h}_i^* \mathbf{h}_i \mathbf{W}_t}{\text{Tr}(\mathbf{h}_i^* \mathbf{h}_i \mathbf{W}_t) - a_i}\right.\right.$$
$$\left.\left. + \frac{\mathbf{h}_i^* \mathbf{h}_i \mathbf{W}_t}{\text{Tr}(\mathbf{h}_i^* \mathbf{h}_i \mathbf{W}_t) - c_i}\right)\right]. \quad (44)$$

The optimal searching step is obtained as

$$\theta = \arg\min_{\theta} f_3(\mathbf{W}_t - \theta \cdot \Delta\mathbf{W}_t), \quad (45)$$

where $\Delta\mathbf{W}_t = \nabla_{\mathbf{W}_t} f_3(\mathbf{W}_t)$ is the searching direction. As a result, after the n-th iteration, the transmit beamforming matrix is updated as $\mathbf{W}_t^{(n+1)} = \mathbf{W}_t^{(n)} - \theta \cdot \Delta\mathbf{W}_t$. Therefore, the optimal transmit beamforming matrix $\mathbf{W}_t^{'\ddagger}$ in the spatial domain and the resultant $P'_{\min,t,norm} = \text{Tr}(\mathbf{W}_t^{'\ddagger})$ of (P6-1) can be then obtained by exploiting Algorithm 1.

If we have $P'_{\min,t,norm} < 1$, we may increase R_{fair} to better utilise the spatial-domain resource. If we have $P'_{\min,t,norm} > 1$, we may reduce R_{fair} because the spatial-domain resource cannot satisfy this high fair-throughput requirement. The binary searching based method can be then exploited for finding the optimal transmit beamforming matrix $\mathbf{W}_t^{\ddagger}$ and the maximum fair-throughput $R_{\text{fair}}^{\ddagger}$, which is detailed in Algorithm 5.

Algorithm 6 SCA Based Algorithm for Solving (P4)

Input: Path loss of $\{\Omega_1, \cdots, \Omega_K\}$; Channel fading coefficients of $\{\mathbf{h}_1, \cdots, \mathbf{h}_K\}$; Transmit power of the H-BS P_t; Noise power of the converter σ^2_{cov}; Duration of the transmission phase T_t; Error tolerance ϵ.

Output: Optimal resource allocation scheme $\{\mathbf{t}^{D\dagger}, \mathbf{t}^{U\dagger}, \boldsymbol{\rho}^{\dagger}, \mathbf{W}_t^{\dagger}\}$ in time- power- and spatial-domain; Maximum uplink fair-throughput $R_{\text{fair}}^{\dagger}$.

1: Initialise the transmit beamforming matrix $\mathbf{W}_t \leftarrow \mathbf{I}/N_t$ in Algorithm 1;
2: Obtain a feasible transmit beamforming matrix $\mathbf{W}_{t,0}^{\ddagger}$ and the resultant minimum total duration $T_{\min}^{D\ddagger}$ of the downlink time-slots by solving (P1-3) based on Algorithm 1;

3: **if** $T_{\min}^{D\ddagger} < T_t$ **then**
4:      Initialise an uplink fair-throughput recorder $R_{\text{fair},0} \leftarrow 0$;
5:      Initialise another uplink fair-throughput recorder $R_{\text{fair},1} \leftarrow 2\epsilon$;
6:      Initialise the transmit beamforming matrix $\mathbf{W}_t \leftarrow \mathbf{W}_{t,0}^{\ddagger}$ in Algorithm 4 for solving (P5-1);
7:      Initialise the transmit beamforming matrix $\mathbf{W}_t \leftarrow \mathbf{W}_{t,0}^{\ddagger}$ in Algorithm 5 for solving (P6);
8:      **while** $R_{\text{fair},1} - R_{\text{fair},0} > \epsilon$ **do**
9:          Update $R_{\text{fair},0} \leftarrow R_{\text{fair},1}$;
10:         Obtain the optimal solution $\{\mathbf{t}^{D\ddagger}, \mathbf{t}^{U\ddagger}, \boldsymbol{\rho}^{\ddagger}\}$ to (P5-1) based on Algorithm 4;
11:         Update $\{\mathbf{t}^D, \mathbf{t}^U, \boldsymbol{\rho}\} \leftarrow \{\mathbf{t}^{D\ddagger}, \mathbf{t}^{U\ddagger}, \boldsymbol{\rho}^{\ddagger}\}$ in Algorithm 5 for solving (P6);
12:         Obtain the optimal solution $\mathbf{W}_t^{\ddagger}$ to (P6) and the resultant uplink fair-throughput $R_{\text{fair}}^{\ddagger}$ based on Algorithm 5;
13:         Update $R_{\text{fair},1} \leftarrow R_{\text{fair}}^{\ddagger}$;
14:         Update $\mathbf{W}_t \leftarrow \mathbf{W}_t^{\ddagger}$ in Algorithm 4 for solving (P5-1) and in Algorithm 5 for solving (P6);
15:      **end while**
16:      Update $\{\mathbf{t}^{D\dagger}, \mathbf{t}^{U\dagger}, \boldsymbol{\rho}^{\dagger}, \mathbf{W}_t^{\dagger}\} \leftarrow \{\mathbf{t}^{D\ddagger}, \mathbf{t}^{U\ddagger}, \boldsymbol{\rho}^{\ddagger}, \mathbf{W}_t^{\ddagger}\}$, $R_{\text{fair}}^{\dagger} \leftarrow R_{\text{fair}}^{\ddagger}$;
17: **else**
18:      No feasible resource allocation scheme.
19: **end if**
20: **return** $\{\mathbf{t}^{D\dagger}, \mathbf{t}^{U\dagger}, \boldsymbol{\rho}^{\dagger}, \mathbf{W}_t^{\dagger}\}$ and $R_{\text{fair}}^{\dagger}$.

C. SCA BASED ALGORITHM

The optimal resource allocation scheme $\{\mathbf{t}^{D\dagger}, \mathbf{t}^{U\dagger}, \boldsymbol{\rho}^{\dagger}, \mathbf{W}_t^{\dagger}\}$ to (P4) can then be obtained by alternatively solving (P5-1) and (P6), which is detailed in Algorithm 6. Note that the existence of a feasible resource allocation scheme to (P4) is validated by solving (P1-2) in Algorithm 1. This may substantially increase the robustness and reduce the complexity of the SCA based Algorithm 6.

V. NUMERICAL RESULTS

In this section, numerical results are provided for characterising the performance of our SCA based multi-dimensional resource allocation algorithms. The transmit power of the H-BS is set to $P_t = 30$ dBm, which is not altered unless specific explanation. The power of the noise incurred by the passband to baseband converter is set to $\sigma_{cov} = -40$ dBm. As shown in Eq.(2), the near-field reference distance of the transmit antennas is set to $d_0 = 1$ m. The RF signal propagating from the transmit antennas to this reference distance suffers from the path-loss of $\Omega_0 = 30$ dB. The path-loss exponent is set to $\alpha = 2$. The duration of the transmission phase is $T_t = 1$ s. We consider a perfect RF-DC energy conversion by letting $\zeta = 1$. Furthermore, uncorrelated Rayleigh block fading is assumed, which remains constant during a single transmission frame T, as depicted in Fig.2, but varies from one transmission frame to another. Both the real and imaginary parts of the channel fading coefficient obey a Gaussian distribution with a zero mean and a unity variance. Without further explanation, the numerical results in this section present the average uplink throughput performance by averaging the randomness incurred by the Rayleigh distributed fading. The error tolerance of the SCA based Algorithms 3 and 6 is set to $\epsilon = 10^{-5}$. The main parameter settings are summarised in TABLE 1.

TABLE 1. Generic parameter settings.

Parameter Description	Value
Duration of transmission phase	$T_t = 1$ s
Transmit power of the H-BS	$P_t = 30$ dBm
Noise power of the converter	$\sigma_{cov}^2 = -40$ dBm
Reference distance	$d = 1$ m
Reference path-loss	$\Omega_0 = 30$ dB
Path-loss exponent	$\alpha = 2$
RF-DC conversion efficiency	$\zeta = 1$
Error tolerance ϵ	10^{-5}

A. CONVERGENCE OF THE SCA ALGORITHM

We firstly study the convergence of our proposed SCA based resource allocation algorithms in Fig.3, which are adopted by the H-BS for supporting the downlink/uplink transmissions of 5 UEs. The H-BS is equipped with 3 antennas. The distances from these UEs to the H-BS are {2, 2, 2, 3, 3} m, respectively. We assume that the UEs have identical downlink throughput requirement $D \in \{0, 0.5, 1.0, 2.0\}$ bit/Hz. When we have $D = 0$ bit/Hz, our IDEN system degenerates to a conventional WPCN. Other parameters are in line with TABLE 1.

Then, we plot the number of iterations[2] against the maximum uplink sum-throughput and fair-throughput in Fig.3. Note that the expected uplink sum-throughput and fair-throughput in Fig.3 are evaluated by averaging the randomness incurred by the Rayleigh distributed fading. As indicated

[2]We only quantify the number of iterations in the SCA based sum-throughput maximisation Algorithm 3 and fair-throughput maximisation Algorithm 6.

in its legend, we study the SCA based resource allocation algorithms with and without the optimal initialisation of the H-BS's transmit beamformer $\mathbf{W}_{t,0}^{\ddagger}$ by solving (P1-1). For the cases without the optimal transmit beamformer initialisation, the equal-gain transmit beamformer $\mathbf{W}_{t,0} = \mathbf{I}/N_t$ is adopted. Furthermore, in the case of WPCN having $D = 0$, the equal-gain transmit beamformer is also adopted for initialising the SCA based resource allocation algorithm.

Observe from Fig.3(a) that all the SCA based resource allocation algorithms having different downlink throughput requirements quickly converge to the maximum uplink sum-throughput by a single iteration or two. Specifically, the algorithms initialised by the equal-gain transmit beamformer converges after two iterations. By contrast, after being initialised by the optimal transmit beamformer $\mathbf{W}_{t,0}^{\ddagger}$ by solving (P1-1), the SCA based resource allocation Algorithm 3 converges to the maximum uplink sum-throughput by only a single iteration.
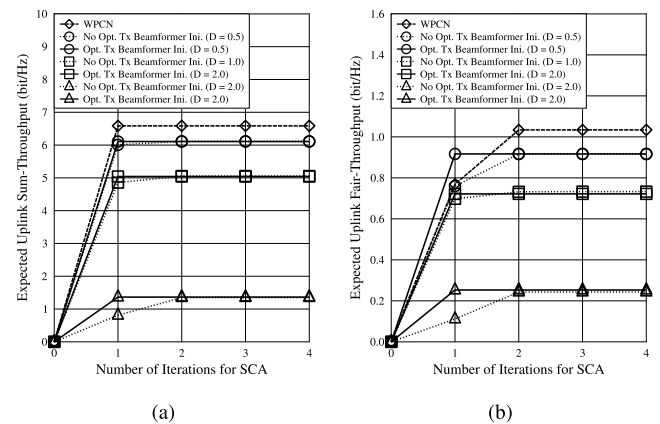

FIGURE 3. The convergence of the SCA based multi-dimensional resource allocation algorithm: (a) Uplink sum-throughput maximisation; (b) Uplink fair-throughput maximisation.

We observe the similar trend from Fig.3(b) that all the SCA based resource allocation algorithms having different downlink throughput requirements converge to the maximum uplink fair-throughput by a single iteration or two. Specifically, the algorithms initialised by the equal-gain transmit beamformer converges after two iterations. By contrast, after being initialised by the optimal transmit beamformer $\mathbf{W}_{t,0}^{\ddagger}$ by solving (P1-1), the SCA based resource allocation Algorithm 6 converges to the maximum uplink fair-throughput by only a single iteration.

The numerical results of Fig.3 validate the low-complexity of our SCA based multi-dimensional resource allocation algorithm, which can be practically invoked by the H-BS for quickly responding to the dynamic information and energy requests of the UEs in both the conventional WPCN and the generic IDEN. Furthermore, the low-complexity algorithm plays an important role in realising the low-latency WIT and WPT in the future IDEN.

B. INDIVIDUAL UPLINK THROUGHPUT

In order to highlight the difference between the uplink sum-throughput and fair-throughput maximisation, we plot the individual uplink throughput attained by 5 UEs in the IDEN during a specific transmission frame, when the sum-throughput and fair-throughput maximisation based resource allocation schemes are invoked, respectively. The H-BS is equipped with 4 antennas. The UEs' downlink throughput requirements are all $D = 1$ bit/Hz. The distances between these UEs and the H-BS are $\{2, 2, 2, 3, 3\}$ m. During this transmission frame, the complex downlink channel fading coefficients are given by the matrix $\mathbf{H}$ of Eq.(46), as shown at the bottom of the next page. By assuming the channel reciprocity, the uplink channel fading coefficients can be represented by $\mathbf{H}^T$. Other parameter settings are in line with TABLE 1.

Observe from Fig.4 that the attainable individual uplink throughput of the UEs varies, when the resource allocation aims for maximising the sum-throughput. For instance, more resources in the time- power- and spatial-domain are allocated to U_3, which may result in a fast growth of the uplink sum-throughput, since it is close to the H-BS and it has a higher channel fading coefficients. However, as depicted in Fig.4, the uplink sum-throughput maximisation results in the unfairness among the UEs in terms of their individual uplink throughput attained. For instance, U_3 attains an uplink throughput as high as 2.96 bit/Hz but U_5 can only attain an uplink throughput of 0.22 bit/Hz.
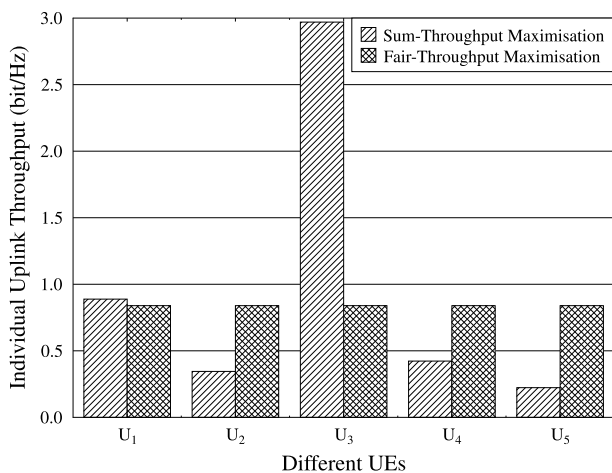

FIGURE 4. The individual uplink throughput of the UEs, when different objectives are invoked for the resource allocation.

The unfairness among the UEs may be addressed by maximising the uplink fair-throughput. Observe from Fig.4 that by maximising the uplink fair-throughput, the multi-dimensional resources are more fairly allocated to all the UEs. As a result, every UE may attain an identical individual uplink throughput of 0.84 bit/Hz. However, the performance of the uplink sum-throughput is inevitably sacrificed.

As a result, the numerical results of Fig.4 demonstrate that the uplink fair-throughput maximisation based resource

allocation scheme is capable of overcoming the doubly near-far effect.

C. MULTIPLE TRANSMIT ANTENNAS

We also study the impact of the transmit antennas on the uplink throughput in Fig.5, where 3 UEs are supported by the H-BS. The distances from these three UEs to the H-BS are $\{2, 2, 3\}$ m, while their downlink throughput requirements are all $D = 1$ bit/Hz. Other parameters are in line with TABLE 1.
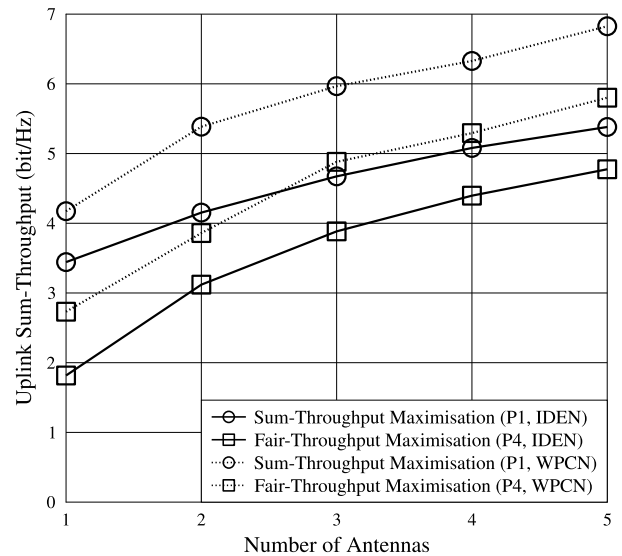
(a)
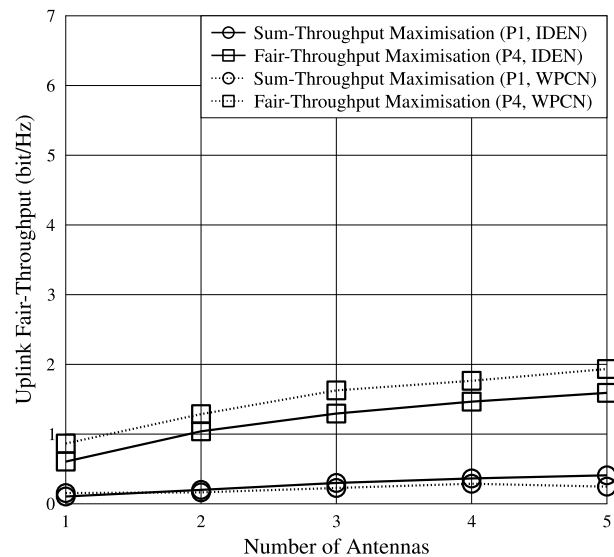
(b)

FIGURE 5. The impact of the transmit antennas on the uplink throughput performance: (a) uplink sum-throughput; (b) uplink fair-throughput.

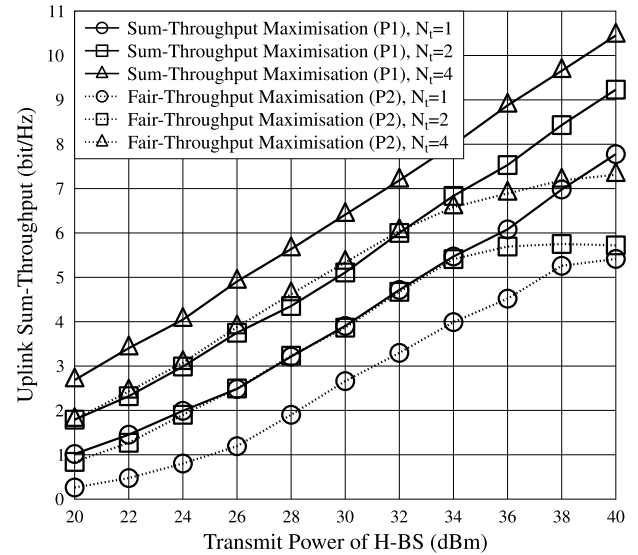We firstly characterise the uplink sum-throughput of both the sum-throughput maximisation oriented and the fair-throughput maximisation oriented resource allocation schemes in Fig.5(a). Obviously, increasing the number

of transmit antennas of the H-BS increases the degree of freedom in the spatial domain. Therefore, the uplink sum-throughput is substantially increased. Furthermore, the fair-throughput maximisation oriented resource allocation scheme sacrifice its sum-throughput performance for achieving the optimal fairness. By letting $D = 0$ bit/Hz, our IDEN degenerates to a conventional WPCN. Since the UEs in a WPCN do not require any downlink data, the downlink resources can be fully exploited for delivering more energy to the UEs. As a result, the uplink sum-throughput of the WPCN outperforms its IDEN counterpart.

We then evaluate the uplink fair-throughput of both the sum-throughput maximisation oriented and the fair-throughput maximisation oriented resource allocation schemes in Fig.5(b). Observe from Fig.5(b) that increasing the number of the H-BS's transmit antennas is capable of enhancing the fair-throughput. Furthermore, the fair-throughput of the sum-throughput maximisation oriented resource allocation scheme is very poor, due to the doubly near-far effect.

The numerical results of Fig.5 demonstrate that the sum-throughput maximisation and the fair-throughput maximisation are a pair of contradictory objectives, which should be carefully balanced in order to satisfy both the H-BS's and the UEs' benefits. These numerical results also validate that increasing the spatial-domain degrees of freedom is capable of improving the throughput performance.
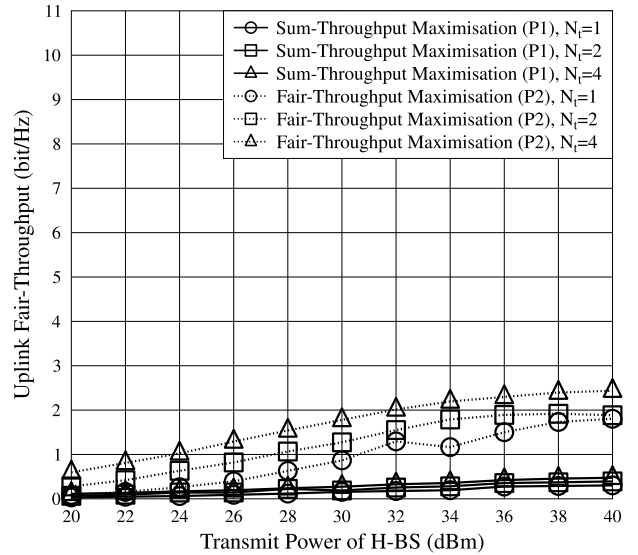
D. TRANSMIT POWER OF THE H-BS

We then plot the transmit power of the H-BS against the throughput performance in Fig.6, when the resource allocation schemes having different objectives are invoked and different number of antennas are equipped at the H-BS. There are 3 UEs supported by the H-BS. The distances from these UEs to the H-BS are {2, 2, 3} m, while their downlink throughput requirements are all $D = 1$ bit/Hz. Other parameter settings are in line with TABLE 1.

The trend observed in Fig.6 is similar to that observed in Fig.5. Both the uplink sum-throughput and fair-throughput increase as we increase the number of antennas equipped at the H-BS. Specifically, observe from Fig.6(a) that the sum-throughput of the sum-throughput maximisation oriented resource allocation scheme almost increases linearly as we increase the transmit power of the H-BS. By contrast, the sum-throughput of the fair-throughput maximisation oriented resource allocation scheme gradually converge as we continuously increase the transmit power of the H-BS. This is because in order to guarantee the fairness, although the

FIGURE 6. The impact of the transmit power on the uplink throughput performance: (a) uplink sum-throughput; (b) uplink fair-throughput.

H-BS has a higher transmit power, the transmit beam may focus more energy to the UEs having poor channels, which largely restricts the growth of the sum-throughput.

Furthermore, observe from Fig.6(b) that the fair-throughput of the fair-throughput maximisation oriented resource allocation scheme steadily increases as we increase

$$\mathbf{H} = \begin{bmatrix} \mathbf{h}_1 \\ \mathbf{h}_2 \\ \mathbf{h}_3 \\ \mathbf{h}_4 \\ \mathbf{h}_5 \end{bmatrix} = \begin{bmatrix} -1.1480 - 0.6003i, & 0.1873 - 2.1384i, & 0.8404 + 0.1240i \\ 0.1049 + 0.4900i, & -0.0825 - 0.8396i, & -0.8880 + 1.4367i \\ 0.7223 + 0.7394i, & -1.9330 + 1.3546i, & 0.1001 - 1.9609i \\ 2.5855 + 1.7119i, & -0.4390 - 1.0722i, & -0.5445 - 0.1977i \\ -0.6669 - 0.1941i, & -1.7947 + 0.9610i, & 0.3035 - 1.2078i \end{bmatrix}. \tag{46}$$

the transmit power of the H-BS. By contrast, the fair-throughput growth of the sum-throughput maximisation oriented resource allocation scheme is quite limited. This is because although the H-BS has a higher transmit power, the power may be beamed to the UEs having good channel quality in order to maximise the sum-throughput by somehow sacrificing the fairness among the UEs.

The numerical results of Fig.6 demonstrate that having a higher transmit power, the H-BS may transfer more energy to the UEs during the downlink transmission, which largely improve the uplink throughput of the UEs.

E. DOWNLINK THROUGHPUT REQUIREMENT

At last, we study the impact of the downlink throughput requirement on the throughput performance of our multi-dimensional resource allocation scheme. We have 3 UEs supported by the H-BS equipped with 4 antennas. The distances from these UEs to the H-BS are $\{2, 2, 3\}$ m. All the 3 UEs have identical downlink throughput requirement D varying from 0 bit/Hz to 4 bit/Hz. Other parameter settings are in line with TABLE 1.

Observe from Fig.7 that as the downlink throughput requirement increases, both the uplink sum-throughput and the fair-throughput reduces. The reason is three-fold:

- In order to satisfy the demanding downlink throughput requirement, more time-domain resources may be allocated to the downlink transmission, which thus reduces the time-domain resources allocated to the UEs for their uplink transmissions.
- More spatial-domain resources (e.g. the transmit beam) is allocated for satisfying the UEs' downlink throughput requirement, which thus reduces the spatial-domain resources used for the WPT in the downlink transmission.

- For the sake of satisfying the increasing downlink throughput requirement, the UE may use a larger portion of the received RF signal for information reception, which thus reduce the amount of energy harvested for powering their uplink transmissions.

Moreover, given the current parameter settings, the H-BS is capable of satisfying the downlink throughput requirement as high as 4 bit/Hz but the uplink transmissions of the UEs are completely sacrificed. In this case, our IDEN degenerates to the pure downlink WIT system. Furthermore, observe from Fig.7 that when we have the downlink throughput requirement lower than 0.5 bit/Hz, the uplink throughput only reduces a little, compared to the conventional WPCN.

The numerical results of Fig.7 characterise the trade-off between the downlink throughput requirement and the uplink throughput performance. Furthermore, they also demonstrate that the H-BS is capable of delivering low-rate downlink data service to the UEs without obviously degrading their uplink throughput. This characteristic can be exploited for delivering the low-rate commanding information to the IoT devices, while powering them for their uplink transmissions.

VI. CONCLUSION

In a H-BS aided IDEN system studied in this paper, the UEs harvest energy and receive information from the downlink transmission of the H-BS and their uplink transmissions are powered by the energy harvested. The optimal resource allocation schemes in the time- power- and spatial domains are obtained by solving the uplink sum-throughput maximisation and uplink fair-throughput maximisation problems. The SCA based algorithms of low complexity are relied upon for iteratively approaching the optimal solutions. The numerical results demonstrate that our SCA based algorithms may effectively return us the optimal resource allocation solutions after only a single or two iterations, which is capable of realising the low-latency WIT and WPT in the IDEN. Furthermore, our IDEN is suitable for the IoT system having asymmetric downlink and uplink traffic load because the numerical results demonstrate that having a downlink throughput requirement lower than 0.5 bit/Hz, the uplink throughput performance may not be substantially degraded.

FIGURE 7. The impact of the downlink throughput requirement on the uplink throughput.

REFERENCES

[1] A. Zanella, N. Bui, A. Castellani, L. Vangelista, and M. Zorzi, "Internet of Things for smart cities," *IEEE Internet Things J.*, vol. 1, no. 1, pp. 22–32, Feb. 2014.

[2] Y. Chen *et al.*, "Energy-autonomous wireless communication for millimeter-scale Internet-of-Things sensor nodes," *IEEE J. Sel. Areas Commun.*, vol. 34, no. 12, pp. 3962–3977, Dec. 2016.

[3] M. Liserre, T. Sauter, and J. Y. Hung, "Future energy systems: Integrating renewable energy sources into the smart power grid through industrial electronics," *IEEE Ind. Electron. Mag.*, vol. 4, no. 1, pp. 18–37, Mar. 2010.

[4] R. F. Atallah, C. M. Assi, and J. Y. Yu, "A reinforcement learning technique for optimizing downlink scheduling in an energy-limited vehicular network," *IEEE Trans. Veh. Technol.*, vol. 66, no. 6, pp. 4592–4601, Jun. 2017.

[5] C. Zhu, V. C. M. Leung, L. Shu, and E. C.-H. Ngai, "Green Internet of Things for smart world," *IEEE Access*, vol. 3, pp. 2151–2162, Nov. 2015.

[6] S. Ulukus *et al.*, "Energy harvesting wireless communications: A review of recent advances," *IEEE J. Sel. Areas Commun.*, vol. 33, no. 3, pp. 360–381, Apr. 2015.
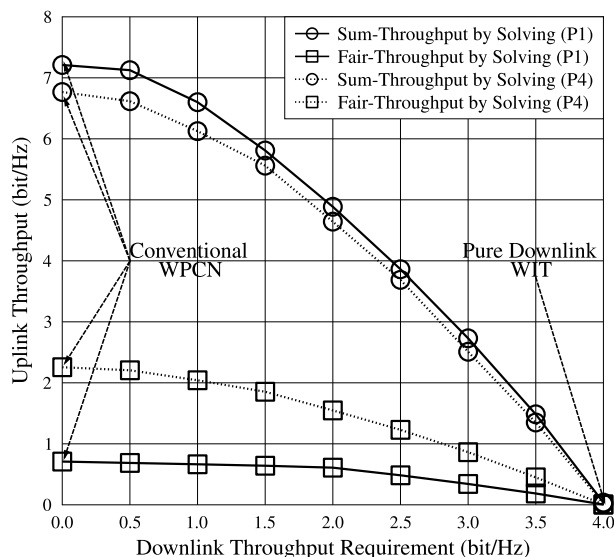
[7] K. Yang, Q. Yu, S. Leng, B. Fan, and F. Wu, "Data and energy integrated communication networks for wireless big data," *IEEE Access*, vol. 4, pp. 713–723, 2016.

[8] U. Muncuk, K. Alemdar, J. D. Sarode, and K. R. Chowdhury, "Multi-band ambient RF energy harvesting circuit design for enabling batteryless sensors and IoT," *IEEE Internet Things J.*, vol. 5, no. 4, pp. 2700–2714, Aug. 2018.

[9] P. N. Alevizos and A. Bletsas, "Sensitive and nonlinear far-field RF energy harvesting in wireless communications," *IEEE Trans. Wireless Commun.*, vol. 17, no. 6, pp. 3670–3685, Jun. 2018.

[10] P. Grover and A. Sahai, "Shannon meets Tesla: Wireless information and power transfer," in *Proc. IEEE Int. Symp. Inf. Theory*, Austin, TX, USA, Jun. 2010, pp. 2363–2367.

[11] D. Niyato, D. I. Kim, M. Maso, and Z. Han, "Wireless powered communication networks: Research directions and technological approaches," *IEEE Wireless Commun.*, vol. 24, no. 6, pp. 88–97, Dec. 2017.

[12] H. Ju and R. Zhang, "Throughput maximization in wireless powered communication networks," *IEEE Trans. Wireless Commun.*, vol. 13, no. 1, pp. 418–428, Jan. 2014.

[13] H. Ju and R. Zhang, "Optimal resource allocation in full-duplex wireless-powered communication network," *IEEE Trans. Commun.*, vol. 62, no. 10, pp. 3528–3540, Oct. 2014.

[14] Y. L. Che, L. Duan, and R. Zhang, "Spatial throughput maximization of wireless powered communication networks," *IEEE J. Sel. Areas Commun.*, vol. 33, no. 8, pp. 1534–1548, Aug. 2015.

[15] H. Chen, L. Xiao, D. Yang, T. Zhang, and L. Cuthbert, "User cooperation in wireless powered communication networks with a pricing mechanism," *IEEE Access*, vol. 5, pp. 16895–16903, 2017.

[16] Q. Wu, M. Tao, D. W. K. Ng, W. Chen, and R. Schober, "Energy-efficient resource allocation for wireless powered communication networks," *IEEE Trans. Wireless Commun.*, vol. 15, no. 3, pp. 2312–2327, Mar. 2016.

[17] T. A. Zewde and M. C. Gursoy, "NOMA-based energy-efficient wireless powered communications," *IEEE Trans. Green Commun. Netw.*, to be published.

[18] W. Huang, H. Chen, Y. Li, and B. Vucetic, "On the performance of multi-antenna wireless-powered communications with energy beamforming," *IEEE Trans. Veh. Technol.*, vol. 65, no. 3, pp. 1801–1808, Mar. 2016.

[19] L. Liu, R. Zhang, and K.-C. Chua, "Multi-antenna wireless powered communication with energy beamforming," *IEEE Trans. Commun.*, vol. 62, no. 12, pp. 4349–4361, Dec. 2014.

[20] M.-L. Ku and J.-W. Lai, "Joint beamforming and resource allocation for wireless-powered device-to-device communications in cellular networks," *IEEE Trans. Wireless Commun.*, vol. 16, no. 11, pp. 7290–7304, Nov. 2017.

[21] L. Yuan, S. Bi, S. Zhang, X. Lin, and H. Wang, "Multi-antenna enabled cluster-based cooperation in wireless powered communication networks," *IEEE Access*, vol. 5, pp. 13941–13950, 2017.

[22] L. R. Varshney, "Transporting information and energy simultaneously," in *Proc. IEEE Int. Symp. Inf. Theory*, Jul. 2008, pp. 1612–1616.

[23] X. Zhou, R. Zhang, and C. K. Ho, "Wireless information and power transfer: Architecture design and rate-energy tradeoff," *IEEE Trans. Commun.*, vol. 61, no. 11, pp. 4754–4767, Nov. 2013.

[24] K. Xiong, B. Wang, and K. J. R. Liu, "Rate-energy region of SWIPT for MIMO broadcasting under nonlinear energy harvesting model," *IEEE Trans. Wireless Commun.*, vol. 16, no. 8, pp. 5147–5161, Aug. 2017.

[25] H. Lee, K. J. Lee, H. Kim, and I. Lee, "Joint transceiver optimization for miso swipt systems with time switching," *IEEE Trans. Wireless Commun.*, vol. 17, no. 5, pp. 3298–3312, May 2018.

[26] K. Xu, Z. Shen, Y. Wang, X. Xia, and D. Zhang, "Hybrid time-switching and power splitting swipt for full-duplex massive MIMO systems: A beam-domain approach," *IEEE Trans. Veh. Technol.*, vol. 67, no. 8, pp. 7257–7274, Aug. 2018.

[27] D. Mishra and G. C. Alexandropoulos, "Transmit precoding and receive power splitting for harvested power maximization in MIMO swipt systems," *IEEE Trans. Green Commun. Netw.*, to be published.

[28] K. Lv, J. Hu, Q. Yu, and K. Yang, "Throughput maximization and fairness assurance in data and energy integrated communication networks," *IEEE Internet Things J.*, vol. 5, no. 2, pp. 636–644, Apr. 2018.

[29] N. Zhao, S. Zhang, F. R. Yu, Y. Chen, A. Nallanathan, and V. C. M. Leung, "Exploiting interference for energy harvesting: A survey, research issues, and challenges," *IEEE Access*, vol. 5, pp. 10403–10421, 2017.

[30] W. Sun, E. G. Ström, F. Brännström, and M. R. Gholami, "Random broadcast based distributed consensus clock synchronization for mobile networks," *IEEE Trans. Wireless Commun.*, vol. 14, no. 6, pp. 3378–3389, Jun. 2015.

[31] Z. Xie, Y. Chen, Y. Gao, Y. Wang, and Y. Su, "Wireless powered communication networks using peer harvesting," *IEEE Access*, vol. 5, pp. 3454–3464, 2017.

[32] J. Hu, L. L. Yang, H. V. Poor, and L. Hanzo, "Bridging the social and wireless networking divide: Information dissemination in integrated cellular and opportunistic networks," *IEEE Access*, vol. 3, pp. 1809–1848, 2015.

[33] L. Liu, R. Zhang, and K.-C. Chua, "Wireless information and power transfer: A dynamic power splitting approach," *IEEE Trans. Commun.*, vol. 61, no. 9, pp. 3990–4001, Sep. 2013.

[34] G. Anjos, D. Castanheira, A. Silva, and A. Gameiro, "Intrinsic secrecy of EGT and MRT precoders for proper and improper modulations," *IEEE Access*, vol. 6, pp. 31317–31326, 2018.

[35] O. Mehanna, K. Huang, B. Gopalakrishnan, A. Konar, and N. D. Sidiropoulos, "Feasible point pursuit and successive approximation of non-convex QCQPs," *IEEE Signal Process. Lett.*, vol. 22, no. 7, pp. 804–808, Jul. 2015.

[36] S. Boyd and L. Vandenberghe, *Convex Optimization*. Cambridge, U.K.: Cambridge Univ. Press, 2004.

JIANJUN YANG received the bachelor's degree in information engineering and automation from Chongqing University, China, in 1994, and the master's degree in communication and information systems from the University of Electronic Science and Technology of China in 2003. He is currently a Lecturer with the Department of Network Engineering, School of Information and Communication Engineering, University of Electronic Science and Technology of China. His research interest is in the domain of resource allocation and optimization in energy harvesting wireless networks and multitier and cooperative cellular networks.

JIE HU (S'11–M'16) received the B.Eng. and M.Sc. degrees from the Beijing University of Posts and Telecommunications, China, in 2008 and 2011, respectively, and the Ph.D. degree from the Faculty of Physical Sciences and Engineering, University of Southampton, U.K., in 2015. Since 2016, he has been with the School of Information and Communication Engineering, University of Electronic Science and Technology of China, China, as an Associate Professor. He has a broad range of interests in wireless communication and networking, such as cognitive radio and cognitive networks, mobile social networks, integrated data and energy communication networks, and communication and computation convergence. His current research is funded by the National Natural Science Foundation of China. He is also in great partnership with industry, such as Huawei and ZTE. He is also a regular TPC member of several prestigious IEEE conferences, such as IEEE ICC and GLOBECOM. He has served for ZTE Communications as the guest editor of the special issue Wireless Data and Energy Integrated Communication Networks.

KESI LV received the B.S degree from the University of Electronic Science and Technology of China, China, in 2016, where he is currently pursuing the master's degree. His research interests include integrated data and energy communication networks and convex optimization.

QIN YU received the B.S. degree in communication engineering from the Chongqing University of Posts and Telecommunications in 1996, and the M.S. and Ph.D. degrees in communication and information engineering from the University of Electronic Science and Technology of China (UESTC) in 2002 and 2006, respectively. She joined the School of Information and Communication Engineering, UESTC, in 2007. From 2007 to 2009, she conducted post-doctoral research with Prof. Z. Qin in information security at UESTC. Her current research interests include data and energy integrated communication networks, wireless communication and information security.

KUN YANG (SM'08) received the B.Sc. and M.Sc. degrees from the Computer Science Department, Jilin University, China, and the Ph.D. degree from the Department of Electronic and Electrical Engineering, University College London (UCL), U.K. He is currently a Chair Professor with the School of Computer Science & Electronic Engineering, University of Essex, leading the Network Convergence Laboratory, U.K. He is also an affiliated professor at UESTC, China. Before joining in University of Essex at 2003, he was at UCL on several European Union (EU) research projects for several years. He has published over 100 journal papers. His main research interests include wireless networks and communications, data and energy integrated networks, and computation-communication cooperation. He manages research projects funded by various sources such as U.K. EPSRC, EU FP7/H2020, and industries. He serves on the editorial boards of both the IEEE and non-IEEE journals. He has been a fellow of IET since 2009.

● ● ●